11-26-2021

Clustered, Stacked and Imbricated Large Coastal Rock Clasts on Ludao Island, Southeast Taiwan, and Their Application to Palaeotyphoon Intensity Assessment

James P. Terry
Zayed University

A.Y. Annie Lau
University of Queensland

Kim Anh Nguyen
National Central University

Yuei-An Liou
National Central University

Adam D. Switzer
Nanyang Technological University

frontiers in Earth Science

ORIGINAL RESEARCH
published: 26 November 2021
doi: 10.3389/feart.2021.792369

Clustered, Stacked and Imbricated Large Coastal Rock Clasts on Ludao Island, Southeast Taiwan, and Their Application to Palaeotyphoon Intensity Assessment

James P. Terry[1]*, *A.Y. Annie Lau*[2], *Kim Anh Nguyen*[3], *Yuei-An Liou*[3] and *Adam D. Switzer*[4]

[1]College of Natural and Health Sciences, Zayed University, Dubai, United Arab Emirates, [2]School of Earth and Environmental Sciences, The University of Queensland, Brisbane, QLD, Australia, [3]Center for Space and Remote Sensing Research, National Central University, Taoyuan, Taiwan, [4]Asian School of the Environment and Earth Observatory of Singapore, Nanyang Technological University, Singapore, Singapore

OPEN ACCESS

Edited by:
Davide Tiranti,
Agenzia Regionale per la Protezione Ambientale (ARPA), Italy

Reviewed by:
Aruna Nandasena,
United Arab Emirates University, United Arab Emirates
Harry Frederick Leonard Williams,
University of North Texas, United States

***Correspondence:**
James P. Terry
james.terry@zu.ac.ae

Specialty section:
This article was submitted to Quaternary Science, Geomorphology and Paleoenvironment, a section of the journal Frontiers in Earth Science

Received: 10 October 2021
Accepted: 28 October 2021
Published: 26 November 2021

Citation:
Terry JP, Lau AYA, Nguyen KA, Liou Y-A and Switzer AD (2021) Clustered, Stacked and Imbricated Large Coastal Rock Clasts on Ludao Island, Southeast Taiwan, and Their Application to Palaeotyphoon Intensity Assessment. Front. Earth Sci. 9:792369. doi: 10.3389/feart.2021.792369

This work investigated the characteristics of a boulder field on the exposed south east coast of Ludao Island (Green Island) in southern Taiwan. Although the region regularly experiences seasonal Pacific typhoons, fieldwork on Ludao was prompted following the double-strike of Typhoon Tembin in August 2012, which followed an unusual looping track and was one of the strongest storms to affect the island in recent decades. In Wen Cuen Bay, large limestone and volcanic clasts (10^3–10^5 kg) occur both as isolated individuals and also grouped into distinct clusters across the gently-sloping emerged reef platform of Holocene age. Some individuals reach megaclast proportions. Observations revealed limited evidence for the production of new coastal boulders by Typhoon Tembin. However, clustering, stacking and notable imbrication of old large clasts provide evidence for multiple high-energy palaeoevents. Stacking and imbrication are significant depositional features, implying that (partial) lifting by wave transport was responsible. Boulders deposited by Typhoon Tembin suggest that storm produced minimum flow velocities of 3.2–5.1 m/s. This range of minimum flow velocity (MFV) values is lower than the 4.3–13.8 m/s range inferred from the pre-Tembin boulders, which indicates that older storm washovers must have been stronger, judging from their ability to stack and imbricate large clasts. One explanation for high upper values of palaeoevent MFVs is that localized funnelling of water flow through narrow relict channels (inherited spur-and-groove morphology, oriented perpendicular to the modern reef edge) concentrates onshore flow energy into powerful confined jets. Support for this hypothesis is the positioning and train-of-direction of the main imbricated boulder cluster at the landward head of one such feature. Geomorphic controls amplifying wave-driven flow velocities across the emerged Holocene reef mean that a palaeotyphoon origin is sufficient for explaining large clast stacking and imbrication, without the need to invoke a tsunami hypothesis.

Keywords: coastal boulders, wave transport, typhoons, tsunamis, stacking, imbrication

INTRODUCTION

Wave-Transported Boulders

Discussions surrounding the origins of coastal boulder deposits have drawn upon field investigations worldwide (e.g., Scheffers, 2004; Mhammdi et al., 2008; Hansom and Hall, 2009; Scheffers et al., 2009; Goto et al., 2010a,b; Switzer and Burston, 2010; Engel and May 2012; Etienne and Terry, 2012; Kennedy et al., 2017; Erdmann et al., 2018). A recent review of possible origins for boulder deposits by Dewey et al. (2021) identified five marine and non-marine mechanisms that might be responsible for their occurrence along shorelines. Of these, boulder deposits attributable to high-energy wave (HEW) action have been found in a variety of coastal settings, such as submarine forereef slopes (Etienne, 2012), beaches (Lau et al., 2015), rocky shorelines (Jones and Hunter, 1992; Paris et al., 2011), coral reef platforms (Nott, 1997; Terry et al., 2013), elevated terraces (Sussmilch, 1912; Ota et al., 2015; Mottershead et al., 2017), and cliff tops (Williams and Hall, 2004; Hall et al., 2006; Roig-Munar et al., 2018). It is understood that considerable energy is required for clast production by waves, i.e. to initially dislodge (pluck or quarry) boulders from rock platforms or reefs (Nott, 2003; Noormets et al., 2004; Morton et al., 2006; Terry et al., 2013). Even for boulders produced by non-marine processes, however, such as rockfall, high-energy flow is needed for their subsequent movement and reorganization (Terry and Goff, 2019). For coastal boulders showing evidence of landward transport, it is normally assumed that wave action of some form was responsible (Noormets et al., 2002; Nott, 2004; Iwai et al., 2019). However, assigning a specific wave process to boulder deposits of unknown origin is often difficult (Bryant and Nott, 2001; Noormets et al., 2002, 2004; Felton and Crook, 2003; Kennedy et al., 2007; Etienne and Paris, 2010; Switzer and Burston, 2010), and therefore this continues to be a worthwhile focus of study.

Boulder Depositional Patterns

Distinctive depositional patterns are often seen in coastal boulders transported by waves. Reported styles of deposition include 1. isolated individual or small numbers of clasts (Frohlich et al., 2009; Terry et al., 2021); boulder fields comprising many clasts that are dispersed across wide areas (Kato and Kimura, 1983; Lau et al., 2018; Kennedy et al., 2019); groups of boulders clustered closely together, sometimes stacked one against another (Terry and Goff, 2019); boulders piled into elongated berms or ridges aligned in shore-parallel orientations (Switzer and Burston, 2010; Cox et al., 2012; Lario et al., 2020). Combinations of such depositional patterns are also possible.

Within boulder clusters and ridges, where clasts have been stacked up against each other, imbrication is sometimes observed (Switzer and Burston, 2010; Scheffers and Kinis, 2014). Imbrication is a distinctive fabric pattern in water-lain sediments, induced by strong and unidirectional currents. Imbricated clasts overlap one another and lean upward in the direction of the current, with their planes of inclination parallel and dipping (Conybeare and Crook, 1982). For imbrication to be recognized, clast morphology should be tabular or ellipsoidal, i.e., with the c-axis significantly less than the a-axis and b-axis.

Although accumulations of pebbles and cobbles in beach environments frequently show imbrication, such patterns are less common in coastal boulder deposits. This is because of the high-energy flow needed to lift or overturn boulder-sized clasts, in order to stack them up against each other in inclined positions. That being said, imbricated coastal boulders have been observed in various locations worldwide. Selected examples include Australia (Bishop and Hughes, 1989; Switzer and Burston, 2010), Greece (Scheffers and Kinis, 2014), Iceland (Etienne and Paris, 2010), Iran (Shah-hosseini et al., 2011), Ireland (Erdmann et al., 2015, 2018; Cox et al., 2019), Malaysia (Master, 2014), Malta (Mottershead et al., 2014), Mexico (Lario et al., 2020) and Morocco (Mhammdi et al., 2008).

Stacked boulder clusters (SBCs), either with or without imbrication (**Figure 1**), deserve special attention, because they can reveal information on wave power and transport processes during the HEW events responsible for their sorting and organization. Several features of SBCs have generated interest, debate and some controversy in coastal geomorphology. In particular, questions have arisen on whether clustering, stacking and imbrication of very large clast sizes (including megaclasts of b-axis > 4.09 m) are key characteristics that can differentiate between tsunami or storm-wave deposition. Some researchers have advocated that such features probably represent the effects of powerful and sustained tsunami flows, and might therefore be used as criteria for determining a tsunami origin (e.g., Young et al., 1996; Bryant and Nott, 2001; Bryant, 2014; Mottershead et al., 2017; Lario et al., 2020). Others disagree, either based on the premise that repeated storm episodes, rather than

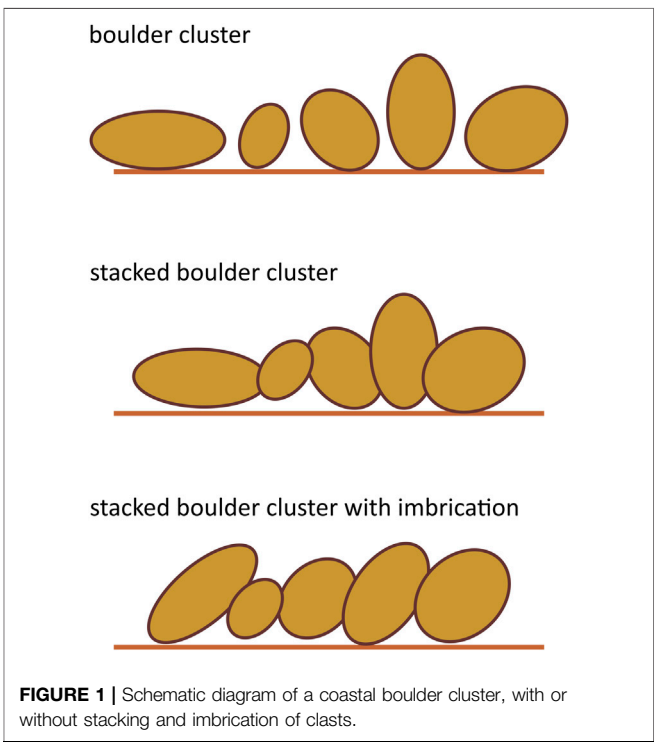

FIGURE 1 | Schematic diagram of a coastal boulder cluster, with or without stacking and imbrication of clasts.

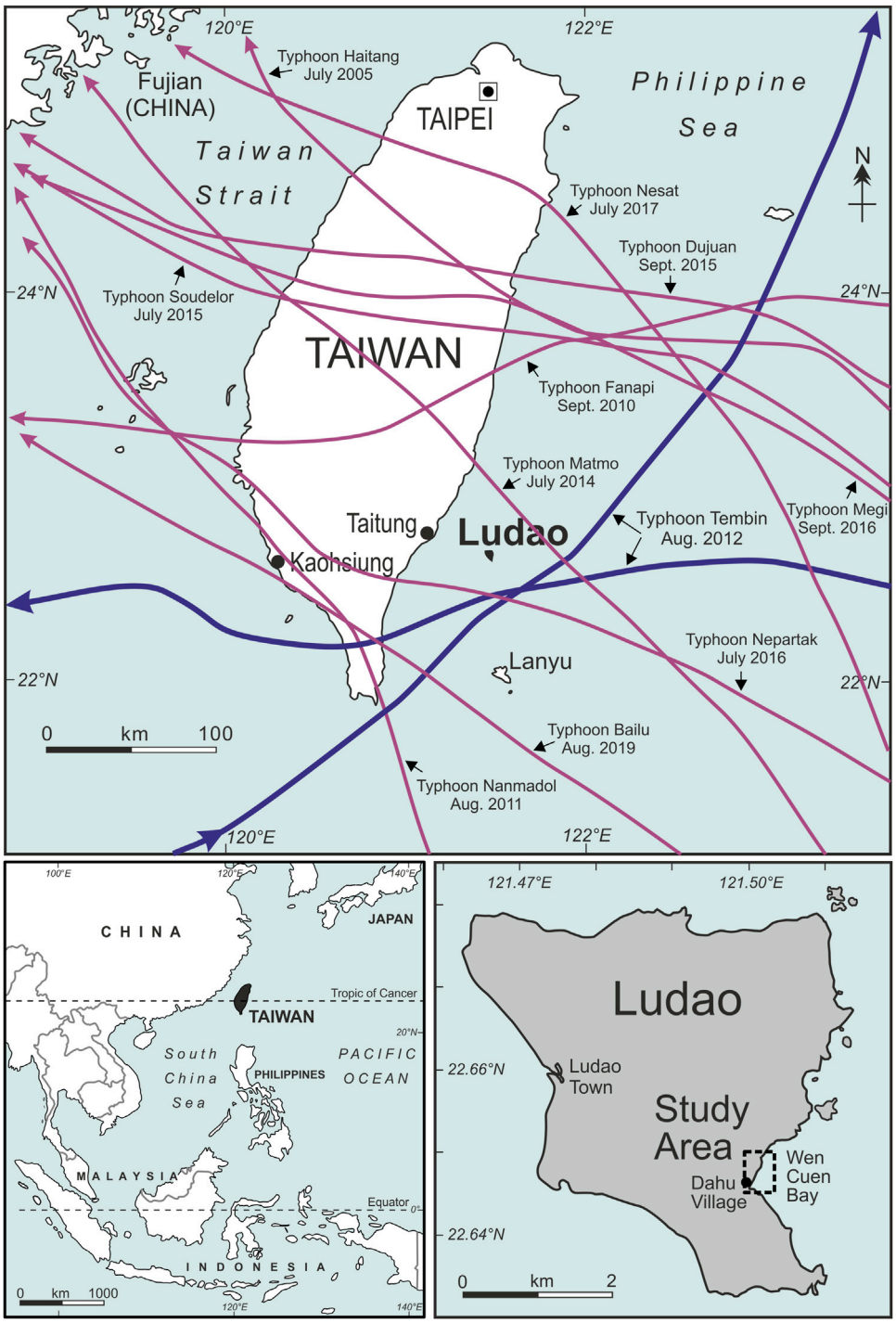

FIGURE 2 | Above: Map of all typhoons that made landfall on Taiwan over the decade 2010–2019. Note especially the storm track of Typhoon Tembin (blue line) that twice struck Ludao in August 2012 and prompted this investigation. Below: Location of Taiwan and the study area on Ludao island.

single tsunami events, are required to arrange large boulders into clusters, stacks and imbricate patterns, or by asserting the competence of high-magnitude storm waves to transport clasts of exceptional size (Hall et al., 2010; Switzer and Burston, 2010; Weiss, 2012; Terry et al., 2013; Hearty and Tormey, 2017; Pepe et al., 2018). In spite of the growing attention, however, the number of reports globally of SBCs containing very large individual clasts (10^3–10^5 kg) remains limited. Likewise, direct evidence on SBCs obtained during or immediately following specific HEW events is understandably lacking, because of the

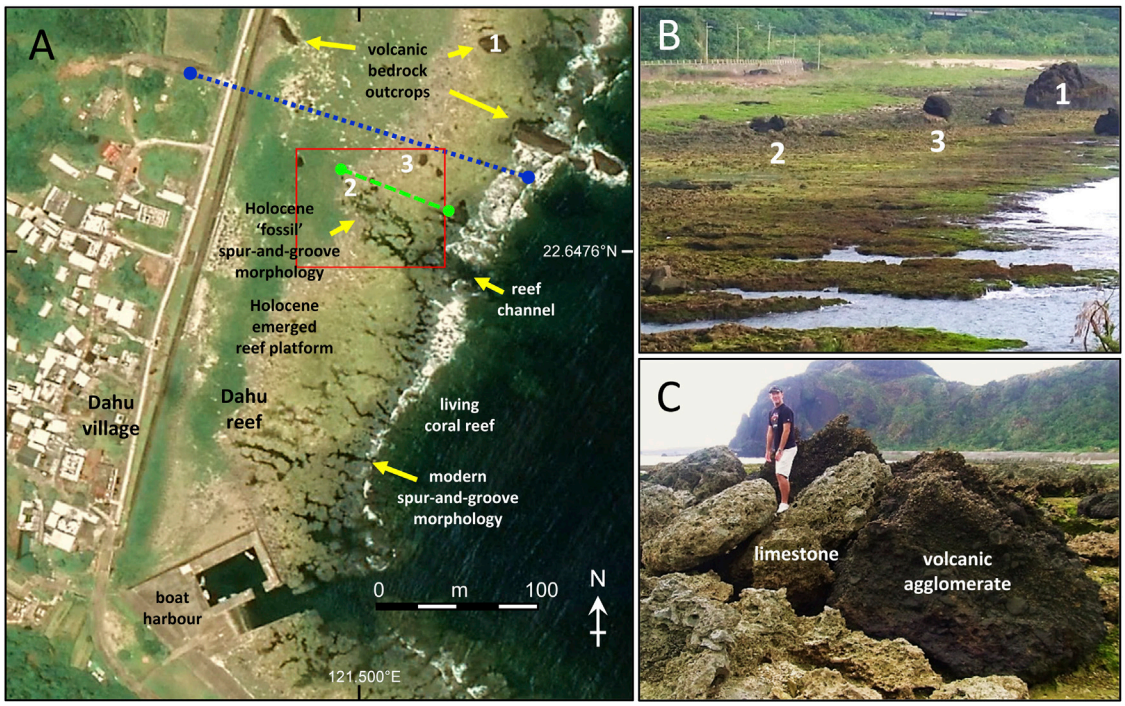

FIGURE 3 | (A): Main site of coastal boulder measurements on the Holocene emerged reef platform near Dahu village in Wen Cuen Bay, south east Ludao, indicating the location of features shown in adjacent images. Several additional boulders were also measured on the reef platform south east of the boat harbour. Note the modern spur-and-groove structure of the living reef edge and similar "inherited" (fossil) structures cutting into the older Holocene surface extending landwards of the shoreline. The dotted blue and dashed green lines approximate the topographic transects surveyed by Inoue et al. (2011) and by the authors, shown in **Figures 4**, **8**, respectively. The red box shows the zoomed area in air photos (**Figure 10**). **(B)**: View looking approximately northward across the coastal platform, showing 1) outcrops of volcanic bedrock (22°38.92′N 121°30.05′), 2) an imbricated cluster of clasts (22°38.88′N 121°30.00′E), and 3) a volcanic megaclast perched on a limestone pedestal 2.3 m above the emerged reef platform (22°38.89′N 121°30.02′E). **(C)**: Close-up view of the imbricated cluster of coastal boulders of mixed volcanic and carbonate lithologies located at position A2 and B2.

rarity of significant tsunamis and extreme storm events, and obvious challenges for field observations of their associated wave processes.

AIMS

Within the context described above, this work investigates the characteristics of a boulder field of very large clasts on the south east coast of Ludao island in south east Taiwan (22°40′N 121°29′E). Historically, eastern Taiwan has experienced only small tsunamis, but the region is regularly exposed to seasonal typhoons (**Figure 2**). Extreme waves have therefore left their sedimentary imprint on Ludao's coastlines. A preliminary reconnaissance visit was made in 2009. A field study was then carried out on Ludao in November 2012, three months after the island was struck by Typhoon Tembin in August 2012, one of the most powerful storms impacting Ludao in recent decades. The resulting coastal boulder data is valuable as it provides an opportunity for pre- and post-typhoon comparisons. The chosen study site is a gently-sloping reef platform of Holocene age. Across this platform, clasts occur both as isolated individuals and also grouped into clusters. Several giant blocks reach megaclast dimensions and exceed 10^4–10^5 kg in mass. Both limestone and volcanic clast lithologies are present. Several clusters notably contain large clasts that are stacked together in a clear imbricate pattern (**Figure 3**).

The specific research questions for this study are:

- What are the size and depositional characteristics of the coastal boulders observed in SE Ludao? Particular focus is on clusters that contain stacked and imbricated boulders.
- Which boulders were moved by waves during the strike of Typhoon Tembin in August 2012? Using available hydrodynamic flow transport equations, what were the estimated wave-generated flow velocities during Tembin?
- Previous unidentified HEW events generated flows of sufficient strength to stack and imbricate some of the largest coastal clasts, but these were left undisturbed by Tembin. How powerful were those past events?
- Were those previous HEW events likely to have been typhoons or tsunamis?
- What do the findings tell us about the coastal vulnerability of eastern Taiwan to extreme events?

The assessment of extreme waves generated by typhoons (tropical cyclones) is fundamental for coastal planning. Yet, such storm events exhibit strong variability on relatively short

timespans, implying that standard statistical methods applied to waves hindcasted or measured at a certain location could lead to uncertain or highly approximate results (Mattioli et al., 2019). This underscores the benefits of comparing a recent typhoon with past HEW events using boulder-inferred data. The findings will also be directly applicable to ongoing debates about the genesis of boulder deposits on rocky shorelines, because previous assertions that clustering and imbrication of large boulders on coastlines are key indicators (possibly unequivocal) of past tsunami events have recently been challenged (Cox et al., 2019). In the local context, both Ludao and nearby Lanyu island (**Figure 2**) are popular 'offshore' destinations for domestic tourism in Taiwan. Lanyu received over 100,000 tourists between 15 and 30 July 2020, for example (Huang, 2020). This work is therefore of relevance concerning risk evaluation for the small offshore islands of SE Taiwan, but also for understanding the broader vulnerability to different types of coastal hazards along Taiwan's 400 km-long exposed mainland east coast facing the Pacific Ocean.

STUDY AREA

Ludao Island

Ludao island, also known as Green Island (綠島 in Chinese), is a small extinct volcanic islet, approximately 3–5 km in diameter (15 km^2 area), lying 35 km off the SE coast of Taiwan in the Philippine Sea. Andesitic pyroclastics and volcanic agglomerates of Miocene–Pliocene–Pleistocene age make up the underlying geology (Geological Map of Taiwan, 1986; Juang and Chen, 1990). The hilly topography rises to a maximum height of 276 m near the island's centre. Ludao is the northern-most volcanic island along the Luzon volcanic island arc, at the boundary of the continuing tectonic collision between the Philippine Sea oceanic plate and the Eurasia continental plate. The island occupies a position between two subduction zones: the Ryukyu and Manila trenches. Although the region experiences frequent seismic activity, only small tsunamis have historically been reported on Taiwan's eastern coastlines (Li et al., 2006).

Ludao has a wet tropical climate, of Af Köppen classification, with annual precipitation and temperature averaging 2,360 mm and 23.4°C, respectively. Monthly mean temperatures range from 19.0°C in January to 26.9°C in July. Taiwan's climate is strongly influenced by the East Asian Monsoon. Seasonal reversals in wind direction are experienced between summer south west and winter north east monsoonal winds (Yen and Chen, 2000). Facing the Philippine Sea (NW Pacific), Ludao is therefore seasonally exposed to north east and easterly winds during the NE monsoon. Data on wave height and period are not available for Ludao, but sea-level monitoring at Chenggong on neighbouring mainland Taiwan provides the nearest data for average wave conditions. At Chenggong, 0.71–1.81 m is the recorded monthly significant wave height (H_s) (calculated as the average wave height of the highest one-third of all waves), and 7.6–8.6 s is the monthly average wave period (Central Weather Bureau (CWB), 2013a).

Ludao's tropical latitude is conducive for the growth of corals, which colonise as fringing reefs around its coastlines. The living reef edge has a typical spur-and-groove morphology in plan form (**Figure 3**). The average tidal range is 0.95 m. Late Quaternary tectonic uplift has caused the emergence of Holocene fossil reefs to different levels around the coast, up to a maximum elevation of 4.5 m in some places, but mostly less than 2.5 m amsl (**Figure 4**, Inoue et al., 2011).

Typhoons

Taiwan lies in one of the most active regions of the NW Pacific's typhoon belt (Chan, 1985). A typhoon is an upper category of migratory tropical storm, with 10-min sustained wind speeds exceeding 118 km/h (64 knots). As noted by Doong et al. (2009), 6.7 typhoons affect Taiwan yearly on average. Taiwan's typhoon season generally lasts from May to October, with the highest typhoon frequency from July to September (Central Weather Bureau (CWB), 2013b; Central Weather Bureau (CWB), 2013c). The typical north-westward track of typhoons near Taiwan (**Figure 2**) means that the main risk of landfall is on Taiwan's eastern coastline. According to the century of historical data over 1911–2010, 74% of the 174 typhoons that made landfall on Taiwan did so by crossing the island's eastern coast (Central Weather Bureau (CWB), 2013d). Significant wave height (H_s) recorded at the Hualien marine buoy station off Taiwan's NE coast during close-tracking typhoons reaches 9–10 m, and occasionally over 11 m, such as during Typhoon Soudelor in 2015 (Huang et al., 2020).

A particular challenge is accurate track forecasting when there is typhoon-to-typhoon vortex interaction (Fujiwhara effects) between simultaneously-occurring systems (Liu et al., 2015; Liou et al., 2019). Interpreting dual-vortex interactions has been advanced by Liou et al. (2016) through the introduction of generalised empirical formulas based on various intensity, rotation and distance parameters. Typhoon enhancement to super-typhoon intensity is also possible through interactions with southwest airflows and cold fronts (Lee et al., 2017), which helps explain the generation of seven super-typhoons in the NW Pacific during the exceptional 2014 season (Liou et al., 2018). Consequently, Ludao island is periodically exposed to typhoon-generated HEW events of much greater energy than typical monsoonal wave conditions.

Typhoon Tembin

Ludao island was heavily impacted by the "double strike" of Typhoon Tembin on 24 and 28 August, 2012 (**Figure 2**). Tembin originated east of The Philippines, then travelled north and later west towards Taiwan. Around midnight local time on 24 August, Tembin passed between Ludao and Lanyu islands for the first time. After making landfall on the southern tip of Taiwan in the morning of the same day, Tembin moved into the South China Sea. Over the next 2 days, Tembin's movement was affected by binary interaction with co-existing Typhoon Bolaven that lay to the north east off southern Japan. This interaction caused Tembin to execute a counter-clockwise loop in the South China Sea. Tembin thereafter resumed a north-eastward track, and passed between Ludao and Lanyu for the second time around midnight on 28 August. Using satellite cloud images, details of the intensification and unusual track behaviour of Typhoon

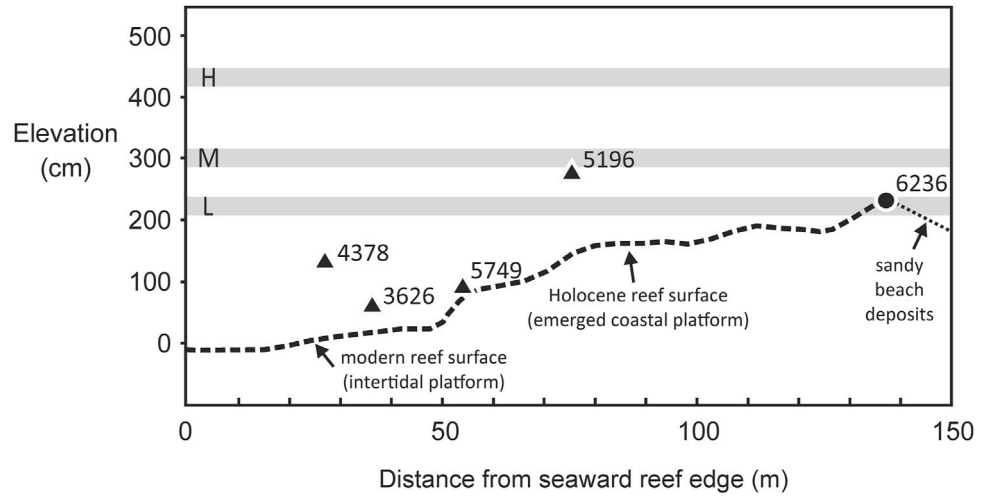

FIGURE 4 | Cross section of surface topography across the coastal limestone platform (Dahu Reef) in Wen Cuen bay. Redrawn and adapted from Inoue et al. (2011). The transect location is shown in **Figure 3**. Black circles or triangles represent elevations of fossil corals sampled by Inoue et al. (2011) from the reef surface at both the study site and elsewhere in eastern Ludao. Calibrated ages (cal yr BP) from radiocarbon dating are indicated. Uplifted Holocene reef terraces at higher levels, exposed in various locations around Ludao, are shown as gray horizontal bars (lower (L), middle (M), and higher (H) marine terraces, from level-and-staff elevations relative to mean sea level (msl)).

Tembin through its interactions with Typhoon Bolaven and two concurrent tropical depressions were explained by Liu et al. (2015).

According to eyewitness accounts, Ludao suffered most damage as Tembin struck for the first time on 24 August. Inhabitants described the typhoon as the worst in history. Tembin produced maximum 10-min sustained wind speeds of 148 km/h (80 knots) in Ludao's vicinity, equivalent to a strong category-3 on the Saffir-Simpson Hurricane Scale, when it initially tracked in an east-to-west direction approximately 20 km south of the island. At Taitung on Taiwan's mainland SE coast, maximum H_s of 8.69 m at wave periods of 12.1 s were recorded (personal communication with the Water Resources Agency of the Ministry of Economic Affairs, Taiwan).

Study Site

During initial reconnaissance in SE Ludao, a coastal boulder field of large clasts in Wen Cuen Bay was identified as a promising site for detailed field investigation (**Figure 3**). The coast is susceptible to typhoons and possibly tsunamis, and it is logical to suppose that the island may have been struck by both types of hazard in the past. The chosen field site is a Holocene-age emerged reef platform near Dahu village. Hereafter the investigated emerged platform is referred to as "Dahu Reef". The surface of the platform is veneered with beach deposits of gravels and sands, and exhibits numerous boulders of both basement volcanic rocks and reef limestone.

In a similar location to our study site, Inoue et al. (2011) surveyed a perpendicular coastal transect landwards from the reef margin across Dahu Reef. The topography shows that the limestone platform generally rises with a gentle slope of approximately 1°, from 0 m amsl at the living reef edge to an elevation of 2.4 m at a distance of 140 m inland (**Figure 4**). At approximately 50–60 m inland from the reef edge is a 0.5 m step up from the modern intertidal zone onto the Holocene emerged reef surface. Coring by Shen et al. (2018) identified that the emerged reef comprises various carbonate lithofacies, including algal-coral boundstones, bioclastic calcrudites and bioclastic-volcanic arenites. Thickness of the emerged reef is up to 15 m overlying volcanic basement. Surface corals on the uplifted reef are mostly encrusting *Isopora palifera*, which also lives at shallow depths on the present living reef (Inoue et al., 2011). Radiocarbon dating by Inoue et al. (2011) of fossil *Acropora digitifera* sampled at 2.34 m amsl yielded a ^{14}C age of 6,091–6,385 cal yr BP (2σ range). More recent uranium-series age-dating of fossil corals suggest that the surfaces of emerged Holocene reef terraces in SE Ludao formed approximately 6,759–5,812 years BP, and that uplift rates have been in the order of 1.2 mm/yr over the past 6,000 years (Shen et al., 2018).

A characteristic feature of the coastal platform is its surface rugosity. Surface roughness includes both natural variation in the marine topography inherited from the former living reef surface and features developed later through subaerial karstification. Some of the pits and depressions occupying the Holocene-age surface are elongate structures, similar in width, orientation and planform geometry to typical spur-and-groove morphology at the modern living reef edge. These elongate depressions cutting into the emerged reef surface are therefore assumed to be "inherited" Holocene (i.e., fossil) spur-and-groove features. Gradual emergence of the Holocene reef above sea level has encouraged rainwater dissolution of the limestone surface, which has overdeepened the fossil spur-and-groove features, and other topographic hollows, to the order of 1 m deep or more.

METHODS

Field Investigations

Field investigations were conducted on the Dahu Reef complex over 5 days in November 2012. Observations were carried out on the emerged platform known to have been inundated by Typhoon Tembin in August that year. Coastal boulders were of two contrasting lithologies: 1) medium to dark grey limestone clasts derived from the reef platform, and 2) dark brown clasts of volcanic agglomerate. The latter match exposures of basement geology on the slopes surrounding the bay, and protruding as vertical outcrops through the reef in several places, being the eroded remnants of volcanic dykes or resistant lava flows (**Figure 3**). Three "concrete clasts" excavated by Typhoon Tembin waves from the structure of the boat harbour at the southern end of the bay gave 3) a third boulder "lithology" .

Coastal boulders were examined and measured. Field methods used to record information were similar to procedures described elsewhere on reef platforms (Terry et al., 2013). Only larger clasts were selected for measurement: boulders with b-axis (intermediate axis) shorter than 1 m were ignored. For each measured clast, the following data were collected: 1) lithology; 2) longitude and latitude coordinates in degrees and decimal minutes (°, ".") using a hand-held Garmin e-trex Venture GPS device with a spatial accuracy of ±5 m; 3) boulder dimensions in metres (m) by tape, recorded as the a-, b-, and c-axis (long, intermediate, and short axis); 4) orientation (directional bearing) of the a-axis in degrees (°) to the nearest ±5° with a hand-held compass; 5) depositional setting, i.e. whether deposited as an isolated clast or part of a cluster, and whether or not stacked together; 6) if imbrication was observed in a stacked cluster, then dip angle of each clast was measured in degrees (°) by clinometer.

The reef profile was surveyed from the reef edge to the main boulder accumulation zone. The distance of individual boulders from the nearest seaward reef edge was not measured, because it cannot be assumed that any individual boulder was originally quarried from this source. The vertical edges of relict channels (relict spur-and-groove morphology) cutting across the emerged platform and other karstic depressions also provide alternative sources for the production of limestone clasts in back-reef locations. For the same reason, fossil corals in limestone boulders were not sampled for age-dating, as this would not provide meaningful data. Only if reef boulders were quarried by past HEW events from the seaward living reef margin can coral mortality age be interpreted as approximating the timing of the event in question. Here, it is possible that limestone clasts might have been sourced from back-reef locations, in which case age-dates would correspond to the older age of their reef-rock composition, and not to the timing of the event that produced them.

Boulder volume (V) and mass (M) were calculated from measured axial dimensions. For clasts with irregular non-geometrical shapes, volumes are typically overestimated by the general calculation $V = a \times b \times c$. Large errors have been established by comparisons between standard geometric calculations for a rectangular prism and accurate clast volumetric measurements by more sophisticated techniques such as photogrammetric 3D modelling, terrestrial laser scanning and differential-GPS (Engel and May 2012; Scicchitano et al., 2012; Gienko and Terry, 2014). To reduce boulder volume overestimation here, therefore, V (m^3) was calculated as the best-fitting ellipsoid:

$$V = \frac{4}{3}\pi\left(\frac{a}{2}\cdot\frac{b}{2}\cdot\frac{c}{2}\right) \quad (1)$$

The ellipsoid calculation is equivalent to $0.52V$ for a rectangular prism of the same axial dimensions. Using this ratio is justified by the findings of Engel and May (2012), who from high-precision DGPS boulder measurements found that average volume is $0.49V$ of an equivalent rectangular prism. The ellipsoidal formula is preferred here even for slab and block-shaped clasts, because clast edges and corners are eroded and irregular.

Clast mass (M) was subsequently estimated from:

$$M = \rho \times V \quad (2)$$

where ρ is clast bulk density: 2.02 t/m^3 for reef limestone, 2.9 t/m^3 for volcanic agglomerate, and 2.4 t/m^3 for concrete. Rock density is assumed from standard values.

Estimating (Palaeo)Wave-Generated Flow Characteristics

Characteristics of flow velocities generated by high-energy waves breaking at the shore and responsible for boulder transport can be inversely modelled, i.e., back-calculated, by applying various published hydrodynamic flow-transport equations. Specifically, minimum values of flow velocity across the reef platform needed to transport individual boulders can be estimated from numerical equations based on clast dimension, mass and assumed mode of transport (sliding, overturning, lifting).

Fluid drag and lift forces must overcome resisting forces (net friction) for a boulder to be set in motion (Noormets et al., 2004). Minimum flow velocity (MFV) required for boulder transport was calculated using the equations developed by Nandasena et al. (2011), which have been widely used since their introduction. **Eq.(3**) and **Eq.4**), modified from Nandasena et al. (2011) (Terry and Malik, 2020), yield the MFV required to initiate each clast's movement by lifting or overturning forces, respectively. These two equations are applied to any limestone boulder assumed to have been initially quarried from the reef edge, cross-cutting channels, or karstic depressions, and then lifted onto the reef flat. The lifting equation should be applied to any boulders that are stacked together in clusters (**Figure 1**), because stacking requires at least partial lifting:

$$u^2 \geq \frac{2\left(\frac{\rho_b}{C_\rho\cdot\rho_w} - 1\right) gc\, cos\theta}{C_l} \quad (3)$$

$$u^2 \geq \frac{2\left(\frac{\rho_b}{C_\rho\cdot\rho_w} - 1\right) gc\left(cos\,\theta + \left(\frac{c}{b}\right) sin\,\theta\right)}{C_d\left(\frac{c^2}{b^2}\right) + C_l} \quad (4)$$

TABLE 1 | Parameters used in hydrodynamic flow transport equations.

Symbol	Parameter
a	a-axis (long axis) of boulder (m)
b	b-axis (intermediate axis) of boulder (m)
c	c-axis (short axis) of boulder (m)
C_d	coefficient of drag (1.95)
C_l	coefficient of lift (0.178)
C_ρ	mixed-fluid density coefficient for seawater containing suspended sediments (1.0[a])
μ_s	coefficient of static friction (0.7)
g	acceleration of gravity (9.81 m/s^2)
u	flow velocity (m/s)
V	volume of boulder (m^3)
θ	slope angle of reef platform (degrees)
ρ_b	density of boulder (2.02 t/m^3 for reef limestone or 2.9 t/m^3 for volcanic agglomerate)
ρ_w	density of sea water (1.025 g/ml)

[a]C_ρ *is a multiplier for clear-seawater density, for conditions of elevated suspended sediment content. See Terry and Malik (2020). Here we assume there is minimal suspended sediment entrainment on the Holocene emerged reef during HEW events affecting Ludao.*

where u is flow velocity (m/s) and all other parameters are as given in **Table 1**.

For the remobilisation during HEW events of pre-existing boulders already present on the reef platform, the required flow velocity may be less, because boulder movement is possible by sliding, which requires less energy than overturning or lifting. Required MFVs for boulder remobilization by sliding are calculated from **Eq. 5**:

$$u^2 \geq \frac{2\left(\frac{\rho_b}{C_\rho \cdot \rho_w} - 1\right) gc\ (\mu_s \cos\theta + \sin\theta)}{C_d\left(\frac{c}{b}\right) + \mu_s C_l} \quad (5)$$

Historical Aerial Photography and Satellite Imagery

Inspection of historical aerial photos and more recent satellite images helps to determine whether or not the positions of coastal boulders have changed, and provides decadal-scale timeframes of wave repositioning, if any, between the dates of successive images. Aerial photos were provided by the Aerial Survey Office of the Forestry Bureau, Council of Agriculture, Taiwan. Low altitude photography was acquired for four dates: December 15, 1979 (2,700 m altitude), June 29, 1989 (1828 m altitude), August 15, 2011 (2,764 m altitude) and October 26, 2014 (3,000 m altitude). Aerial photos were imported for display into QGIS software. Satellite images spanning 2005 to 2019 were examined using Google Earth. The earliest satellite image with a sufficiently fine resolution to pick out individual boulders on Dahu Reef platform was dated January 2005.

Individual large boulders on aerial photos and satellite images were identified by comparing their shapes to boulder details logged during fieldwork. However, the clarity of aerial photos was insufficient for the identification of small objects. Attention was therefore focused on only the largest individual boulders (a-axis >3 m), or clusters of boulders, which could be confidently relocated between successive images. If any clasts were positively identified to have changed position, then information was recorded on the distance and direction of displacement.

OBSERVATIONS AND RESULTS

Boulder Origins, Depositional Settings and Characteristics

Megaclasts

Several exceptional volcanic boulders of megaclast size (Terry and Goff, 2014) are deposited on Dahu Reef (**Figure 5**). The largest clasts of all are standing on remnant pedestals of reef limestone, indicating that (parts of) the Holocene reef was once at least 2.5 m higher than present level (**Figures 3B3**, **5**). The largest measured volcanic megaclast has impressive dimensions: 6.6 × 4.6 × 3.3 m, weighs approximately 150 t (metric tonnes), and is perched in a "delicately balanced" position (Scheffers and Kinis, 2014). It is doubtful that such volcanic megaclasts have been wave-transported, and so are not included in hydrodynamic flow calculations. Although the manner of their deposition in the coastal zone is debateable, it is likely they originated as rockfall from elevated exposures on the steep slopes surrounding the bay, especially recognising that Taiwan is prone to seismic activity. Momentum would have been sufficient for volcanic megaclasts dislodged by earthquakes or gravity-driven instability to roll into their current coastal positions. Inoue et al. (2011) mapped these volcanic deposits in the coastal zone as "talus", likewise alluding to their slope origin.

The largest 150 t volcanic megaclast (**Figure 5**) has been responsible for the formation of its supporting limestone pedestal, by protecting this Holocene reef remnant from rainwater solution. The preserved pedestal with the clast balancing on top is therefore evidence that wave action has not repositioned this megaclast during at least the span of the late Holocene. The duration of stability is inferred from the relative lowering rate of the surrounding exposed limestone platform: an estimated solution rate of 1 mm/yr (Terry, 2005) suggests at least 2,500 years of surface lowering during which the volcanic megaclast has remained immobile.

The largest limestone clast sourced from the reef itself is also of megaclast proportions (5.9 × 4.4 × 2.6 m) and weighs approximately 73 t. It is deposited at approximately the high tide line (**Figure 5**). As this clast is neither *in situ* nor perched on a supporting pedestal, it has presumably been wave-transported.

General Boulder Characteristics

Data on 37 large coastal boulders was recorded at the Dahu Reef study site (**Table 2**). Maximum measured boulder volume and mass were impressive: up to 36 m^3 (73 t) for limestone clasts, and 41 m^3 (118 t) for volcanic clasts. Clasts shapes fall within different categories using the system of Blott and Pye (2008) for defining three-dimensional (3D) form. In general, limestone clasts are mostly slabs or flat

FIGURE 5 | The largest coastal boulders observed on Dahu Reef. Above: Two views of a volcanic agglomerate megaclast (6.6 × 4.6 × 3.3 m) weighing approximately 150 t, perched on a pedestal of Holocene reef above the surrounding platform (22°38.89′N 121°30.02′E). This individual is not believed to be a wave-transported clast. Because the pedestal of limestone is protected from rainwater solution by the volcanic boulder resting on top, the highest point of the pedestal now stands 2.5 m higher than the surrounding reef level. Below: The largest limestone clast observed at the study site (22°38.89′N 121°30.03′E) is similarly of megaclast proportions, measuring 5.9 × 4.4 × 2.6 m and weighing approximately 73 t. Limestone clasts have been quarried from the reef by wave action and subsequently wave-transported to their current locations, by one or more past HEW events.

TABLE 2 | Summary measurements of coastal boulders on Dahu Reef, southeast Ludao.

Boulder parameter	Mean	Range
Limestone clasts (n = 25)		
Shape	flat block[a]	plate–slab–flat block–sub-equant block–blade
a-axis (long axis) (m)	2.9	1.1–5.9
b-axis (intermediate axis) (m)	2.1	0.8–4.4
c-axis (short axis) (m)	1.0	0.1–2.6
Volume (m^3)	4.5	0.2–36.0
Mass[b] (tonnes)	9.0	0.2–72.8
Volcanic boulders (n = 9)		
Shape	sub-equant block[a]	flat block–equant block–elongate block
a-axis (long axis) (m)	3.7	1.3–6.1
b-axis (intermediate axis) (m)	2.4	1.1–4.3
c-axis (short axis) (m)	1.8	1.0–2.9
Volume (m^3)	12.4	0.8–40.5
Mass[b] (tonnes)	35.9	2.3–117.5

[a]*Modal class. Three-dimensional form following the categorisations of Zingg (1935) and Blott and Pye (2008).*
[b]*Mass based on measured density of 2.02 and 2.90 t/m^3 for limestone and volcanic lithologies, respectively.*

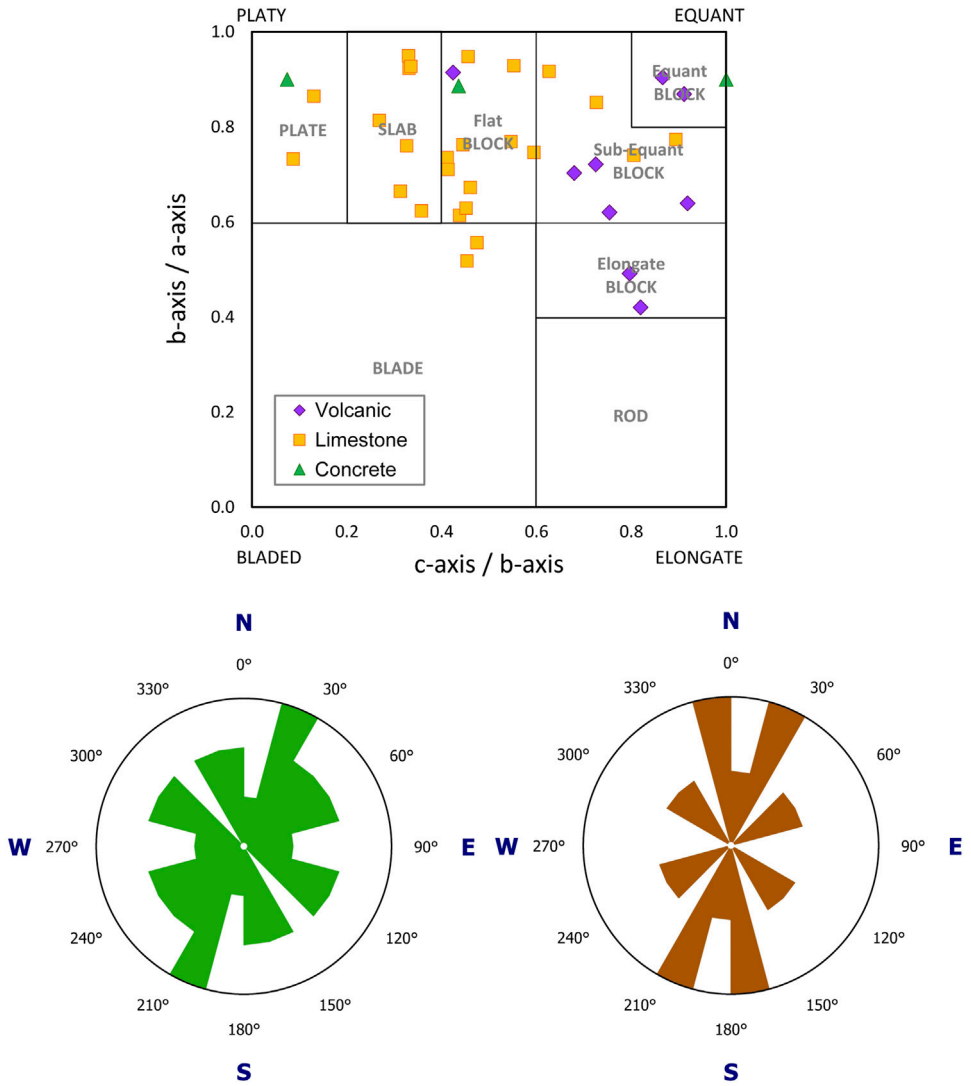

FIGURE 6 | Above: Measured boulder 3D form, plotted on a Zingg diagram (Zingg, 1935; Blott and Pye, 2008). Below: Orientation of long-axes for limestone **(left)** and volcanic **(right)** clasts.

blocks, whereas most volcanic clasts have sub-equant block or elongate block shapes (**Figure 6**). Edge-rounding by attrition and abrasion over long periods has given boulders mostly a subangular to sub-rounded appearance. Data on boulder long-axis orientations reveal non-random patterns. Modal directions are similar for both types of clast lithology, with N-NNE to S-SSW being the preferred orientation (**Figure 6**). Such orientations suggest past wave action has been responsible for clast alignment (see below).

Wave-Transported Boulders

For volcanic boulders below megaclast size on Dahu Reef, these may similarly have been delivered into the coastal zone as rockfall debris, or alternatively may have been eroded by waves from several volcanic outcrops that protrude through the limestone reef (**Figure 3B1**). For those volcanic boulders cemented to the reef platform or perched on limestone pedestals, no recent transport has occurred. Even for volcanic boulders that are detached from the reef, however, convincing evidence of wave transport was not necessarily found. Yet, for several volcanic boulders, past wave transport is indicated. Evidence for this is 1) remnants of limestone cement on upper surfaces, suggesting they have been overturned (**Figures 7A,B**), 2) attachments of reef limestone where a volcanic boulder has been torn from its original reef foundation (**Figures 7C,D**), 3) the similar modal class of a-axis orientations (NNE–SSW) for both volcanic and limestone clasts (**Figure 6**)

For reef-derived limestone boulders, it is feasible that all have been transported by HEW events in the past. In a cluster of mixed lithology boulders at the head of a cross-cutting relict reef channels (**Figure 3C**), strong evidence of wave organisation is the stacking and observed imbricate pattern (see below). That

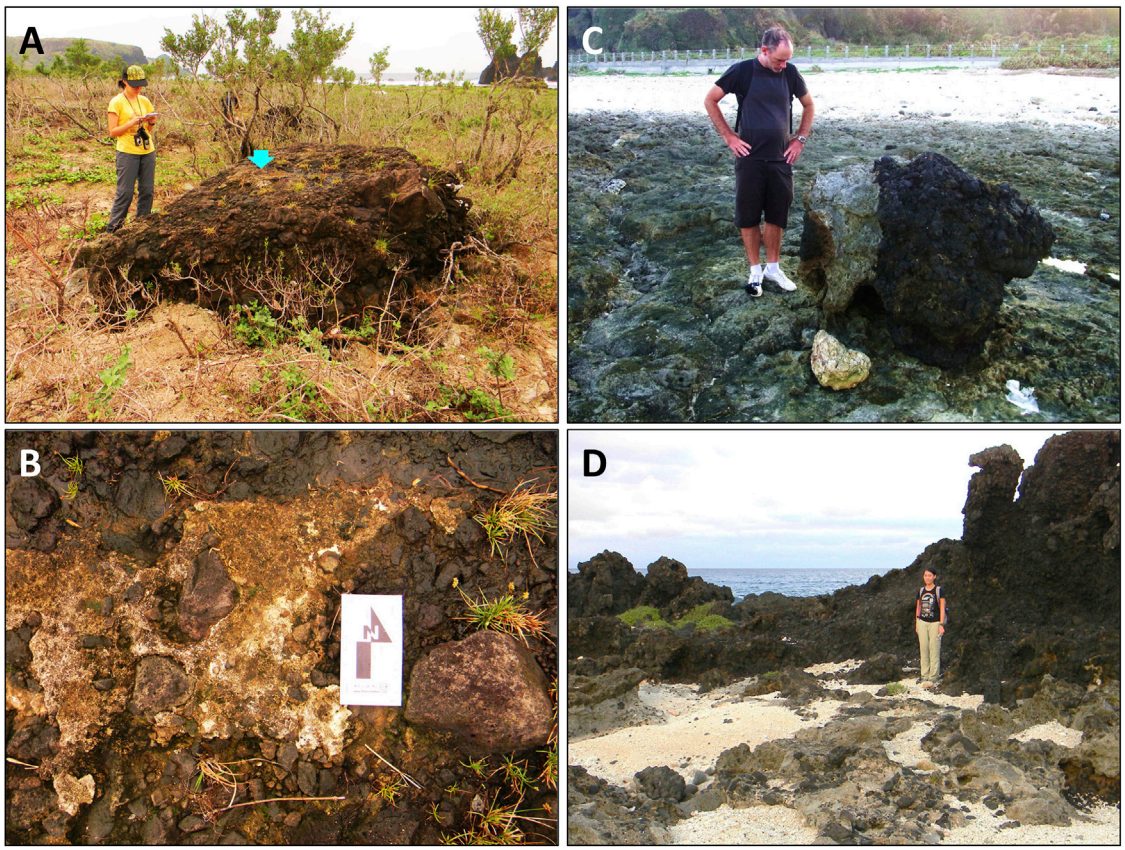

FIGURE 7 | Left: Large volcanic boulder (2.8 × 2.6 × 1.1 m, 12.0 t) with a veneer of limestone cement on its upper surface, as indicated by the blue arrow **(A)** and seen close up **(B)**. Right: a volcanic boulder (4.2 t) with an attachment of limestone **(C)**, showing it was originally attached to the reef but has later been torn off its foundation by past wave action. The person in **(D)** is standing at the source location of this boulder. Both examples are evidence that some of the volcanic clasts on Dahu Reef have been transported (overturned) by past HEW events.

being said, however, indication of boulder stability over considerable periods before present is the dissolution by rainwater of the upper surface of most limestone clasts that are lying flat, which has produced notable pitting. Surface karstification thus implies that many limestone clasts have not recently been overturned by wave action. Air photo and satellite imagery verified this finding (see below).

Clustering, Stacking and Imbrication

One of the remarkable features observed on Dahu Reef is the clustering, stacking and imbrication of a set of large clasts accumulated in a reef-surface topographic depression at the head of an elongate remnant spur-and-groove feature (**Figure 8**). The relict channel network has a digitate plan morphology, generally oriented in a NW–SE direction (i.e., perpendicular to the reef edge). It extends approximately 60 m landwards across the Holocene emerged reef, continuing beyond the end of the modern 10 m-wide surge channel that cuts into the seaward reef edge (**Figure 3A**). The stacked boulder clusters (SBCs) are of mixed lithology, comprising clasts of both reef limestone and volcanic agglomerate.

The cluster of boulders comprised 20 individual clasts with b-axis longer than our chosen 1 m threshold measurement value, as well as many other unmeasured smaller boulders of both volcanic and limestone lithology. Within the cluster, 18 clasts were stacked together (**Figure 9**), i.e., leaning against one another with clast a-b faces inclined. Dip angles ranged from 8 to 48°. Owing to irregular clast shapes and variety of 3D form (**Figure 6**), not all stacked clasts overlapped in a regular fashion to produce a clear imbricate pattern. However, ten boulders were recognisably imbricated, with an average imbricate dip angle of 27°. Most of these boulders dip to the east, i.e., imbricated in a landward direction (**Figures 9C–E**), with some exceptions that dip NE-SE at lower dip angles (**Figure 9A**). One clast dips SW (**Figure 9B**, ID#354, 8.0 t), and a smaller boulder dips northward (ID#345, 2.6 t).

The main cluster can be divided into five separate stacks with two to four overlapping boulders in each stack (**Figure 9**). Boulders in these stacks are leaning against or sitting on top of one another, with the end member either lying flat or at an angle on the karstified surface. The stack that is most clearly imbricated has a large volcanic clast at its landward end, with three eastward-dipping limestone clasts

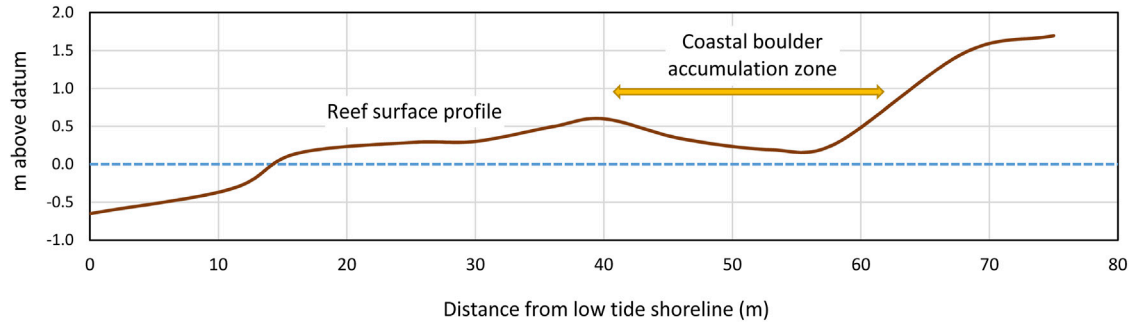

FIGURE 8 | Surveyed reef-platform surface topography (see **Figure 3A** for transect location). Note the back-reef depression that acted as the main accumulation zone for the wave-deposited cluster of stacked and imbricated clasts (**Figure 8**).

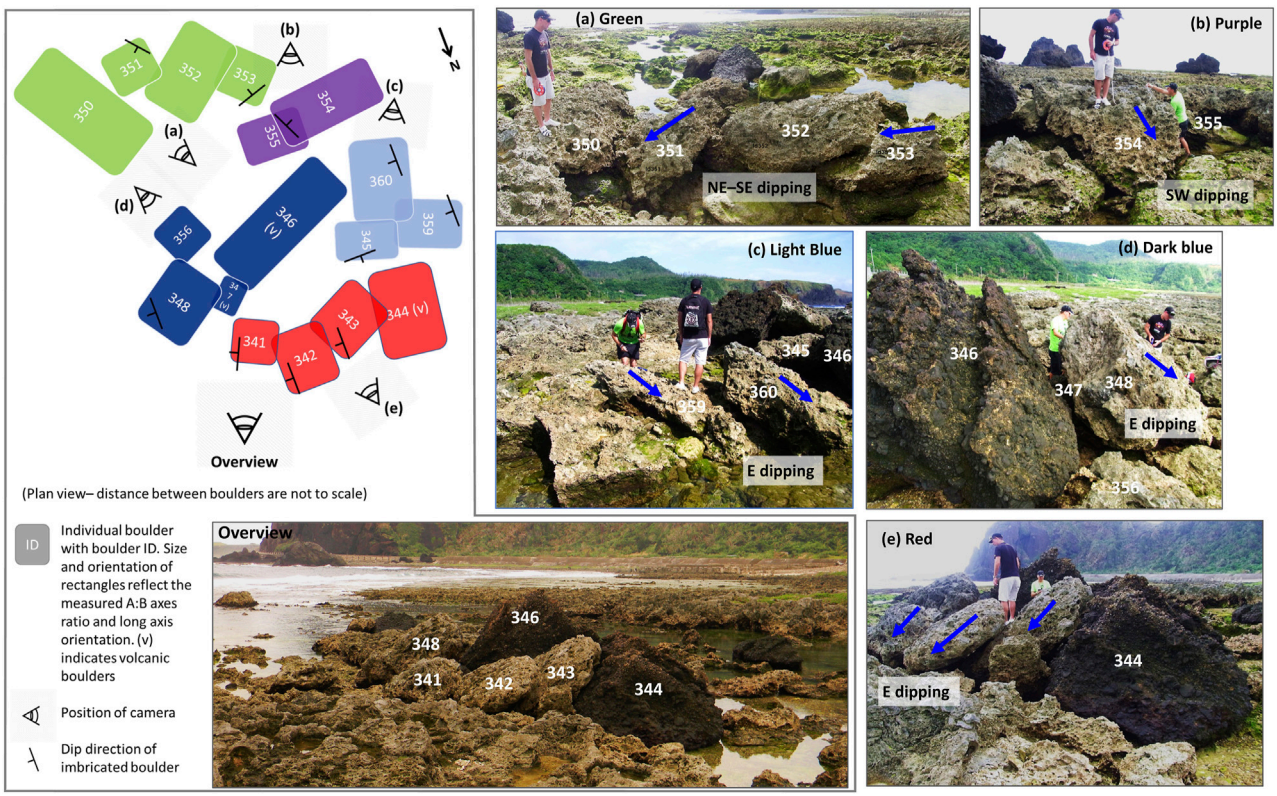

FIGURE 9 | Different views of the cluster of large coastal boulders of mixed lithologies (limestone and volcanic), deposited at the head (i.e., landward end) of remnant spur-and-groove depressions that today form shallow tidal pools on the emerged Holocene platform of Dahu Reef. The location of this cluster is shown in **Figure 3B2**. The top-left illustration shows the arrangement of boulders in this cluster. Most boulders are overlapping or leaning on another individual (indicated by a rectangle partly overlaying another in the illustration). Ten boulders are imbricated, or leaning on other clasts with an inclined/dipping surface. Dip directions are indicated by a dip symbol on rectangles, and by blue arrows in the photos. Boulders are colour-coded in the plan view illustration to indicate which photo **(A–E)** and which stack of clasts they are in.

leaning against it (the red stack in **Figure 9**). This imbrication suggests that the 'anchor' clast at the landward end of the stack was deposited first, while those in more seaward positions were subsequently deposited during the same event or by later HEW events.

Another large volcanic clast #346 (32.4 t) is situated in the centre of the main cluster between two separate stacks (the dark and light blue stacks in **Figure 9**). The limestone boulder at the landward end (#359, 2.8 t) rests on a step in the reef flat at an inclined angle, resulting in an eastward-dipping surface.

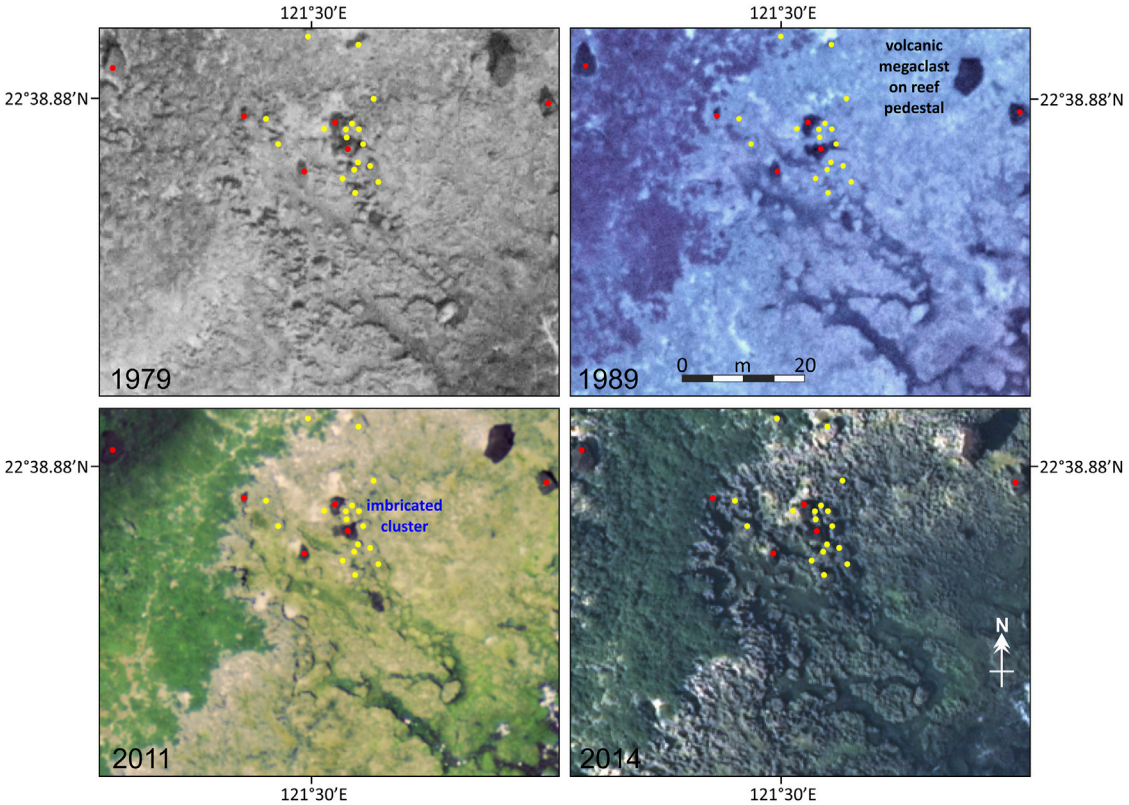

FIGURE 10 | A sequence of aerial photos and satellite images spanning nearly 4 decades, showing details a section of Dahu Reef approximately 70 m × 60 m in area. The location of the area covered by the images is indicated in **Figure 3A**. The stacked boulder clusters (SBCs), some of which display imbricate patterns, are located at the head of a relict channel network (remnant spur-and-groove formation) that forms relatively low-lying depressions on the reef platform. Comprising the group are clast lithologies of both volcanic agglomerate (red dots) and reef limestone (yellow dots). A selection of other measured isolated clasts is also shown. Comparison between the images shows no significant evidence of wave transport of any measured large clasts (a-axis >3 m) on Dahu Reef, either by Typhoon Tembin in 2012 or by typhoons in earlier decades since 1979.

Another imbricated limestone clast was deposited on it at a similar dipping angle, which is in turn overlain by a slightly smaller, northward-dipping clast (#345, 2.6 t). These three limestone clasts form the light blue stack (**Figure 9C**). In the dark blue stack (**Figure 9D**), an eastward-dipping clast (#348, 9.6 t) at the seaward side of the volcanic clast is leaning on a smaller boulder (#347, 2.3 t) that is sandwiched between the two. These two stacks of boulders in close proximity, although disconnected, show a sequence of boulder deposition. The landward-most eastward-dipping boulders were transported by an older event (or events), while the larger boulders at the seaward ends were deposited later. We determine that limestone clasts #359 and #360 were deposited before the largest volcanic clast #346: if the volcanic clast had been deposited first, then it would have blocked the transport path of limestone boulders from the east. The green and purple stacks of limestone boulders (**Figures 9A,B**) are not clearly imbricated, because the boulder surfaces dip in a way that is controlled by their irregular shapes and by the reef topography. It is therefore important to exercise caution regarding the dip direction in such cases. Nonetheless, the arrangement of the boulder train again helps to understand the depositional order, with boulders at the seaward (SE) end likely deposited later.

As the study coastline is exposed to regular typhoons, it seems improbable that all coastal boulders present were deposited by a single event. Similarly, we suggest that individual clasts in the large boulder cluster may not have been stacked together at the same time, although this remains a possibility. However, features of the depositional configuration of the SBCs, including a-axis orientations, common dip-directions and seaward–landward direction of the "trains-of-imbrication" (**Figures 9**, **10**), offer convincing evidence to suggest that the strongest waves during past HEW events approached Ludao from the SE quadrant.

Historical *Versus* Recent Boulder Transport

Evidence From Historical Imagery

Aerial photographs and satellite images for 1979, 1989, 2011 and 2014 were examined for any historical boulder movement on the Dahu Reef platform, or as a result of Typhoon Tembin in 2012 (**Figure 10**). Different heights of air photography, angles of image capture, shadows cast by Sun angle, image resolutions, and high tide levels at the times of image acquisition, limited the accuracy of pinpointing the locations all boulders measured in the field

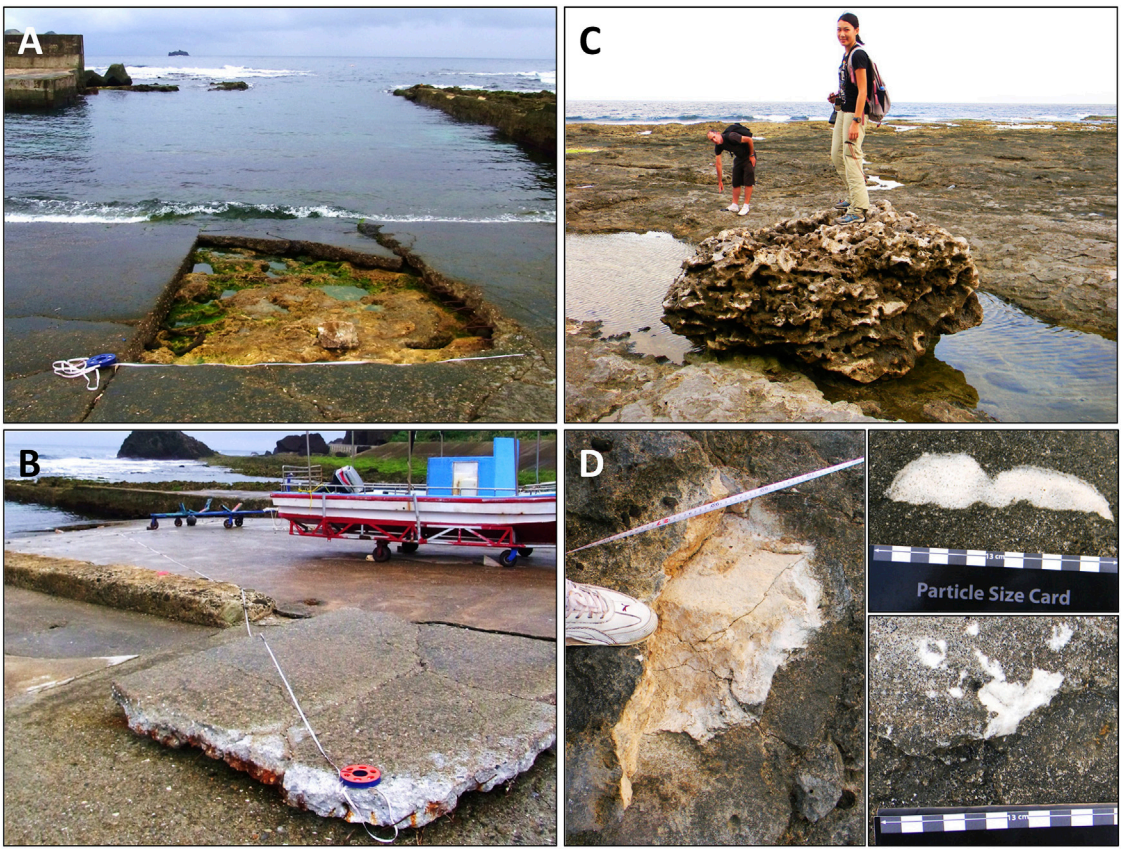

FIGURE 11 | Left: Damage to the apron of the boat ramp **(A)** at the fishing harbour in Wen Cuen Bay caused by Typhoon Tembin in August 2012. Seen in **(B)** is the 2.8 t concrete slab plucked out and rafted upslope by 20 m in a northwest direction. Right: Pre-existing 7.3 t limestone boulder **(C)** situated at the landward edge of a depression/tidal pool, which was remobilised during Typhoon Tembin. Fresh scars are present on all surfaces of the boulder, indicating overturning mode of wave transport. The person in the background is indicating various percussion marks on the reef surface **(D)** caused by impact of this boulder as it was transported across the reef platform. The farthest visible impact mark was found 30 m seaward, with the transport direction towards the southwest.

across all time stamps. Nonetheless, it was possible to identify 1) volcanic clasts that stood out clearly as dark objects against the lighter background of the reef platform, 2) the largest of the limestone clasts (a-axis >3 m), and 3) the cluster of stacked boulders at the head of the fossil spur-and-groove depression. The sequence of images revealed little evidence for the production of new large clasts (>3 m) between 1979 and 2014. Likewise, reworking of pre-existing large clasts over this timeframe by typhoons, including Typhoon Tembin in 2012, has been minimal. This supports the idea that the HEW event(s) responsible for large clast production, clustering, stacking and imbrication on Dahu Reef were pre-historical events, although their timing cannot be determined.

Typhoon Tembin

Fieldwork on Dahu Reef revealed no evidence for any change in the SBCs described above resulting from Typhoon Tembin in August 2012. Moreover, there was little production of new large limestone boulders (>10^3 kg), in spite of Tembin being one of the strongest storms to impact Ludao in recent decades. No large limestone clasts comprised fresh corals, which would have indicated recent sourcing from the living reef edge. If Tembin waves had quarried new limestone clasts from back-reef depressions, then recently-living corals would not be part of the clast fabric. However, fresh boulder faces would nonetheless reveal where clasts had broken away from the limestone bedrock. This was not the case. Fresh percussion marks were observed on some boulders, likely showing *in situ* collisions from saltating smaller boulders or cobbles.

At the south end of Dahu Reef, three "concrete clasts" (max. 8.1 t) were broken from the wharf structure around the boat harbour at the southern end. One slab (**Figure 11B**, 2.8 t) was plucked from the boat-ramp apron and rafted 20 m upslope. Three freshly overturned limestone boulders were also identified on the adjacent reef, south of Wen Cuen Bay. The largest one measured 2.50 × 1.85 × 1.49 m (7.3 t) (**Figure 11C**). The surface of this boulder is considerably weathered but also displayed fresh percussion marks on all surfaces, suggesting it was reworked on the platform itself, instead of being newly quarried from the submerged reef by the Tembin event. Also, the nearby presence of fresh chatter marks and gouges on the reef platform (**Figure 11D**) indicate

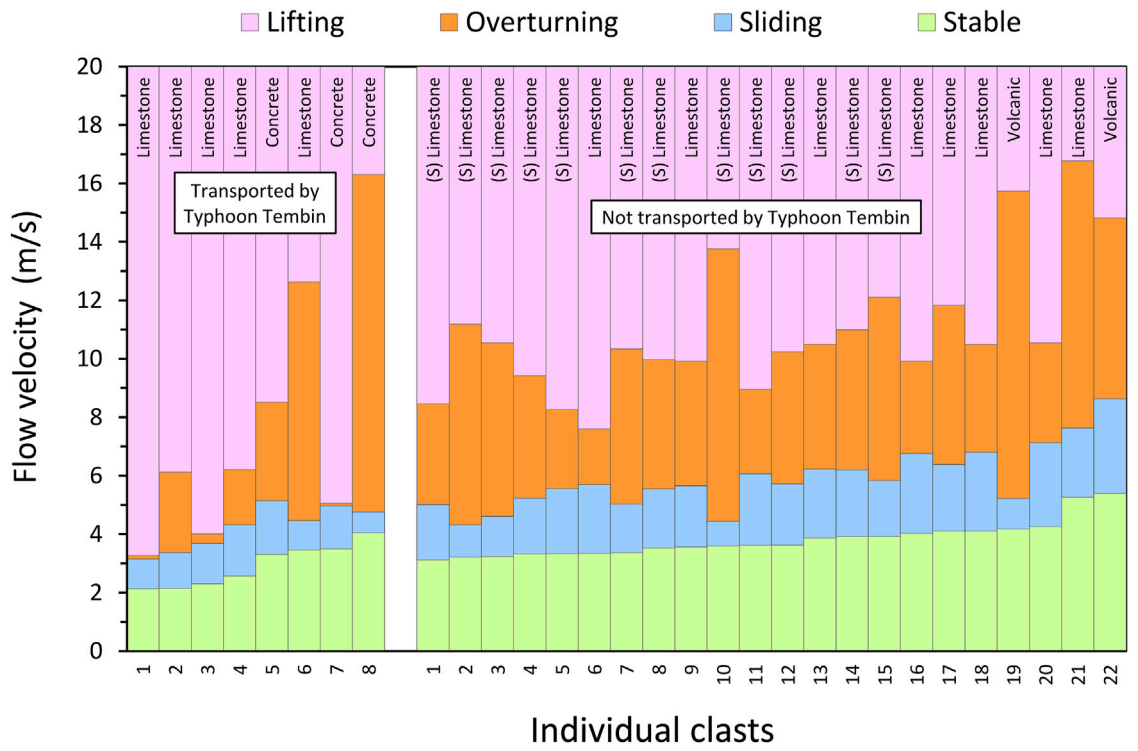

FIGURE 12 | Transport histogram for coastal boulders at the Dahu Reef study site. Only those clasts for which past wave-transport is certain are included. The horizontal axis arranges individual clasts in ascending rank according to the flow velocity needed before stability thresholds (green shading) are exceeded, so allowing the initiation of transport. The left vertical axis displays the ranges of flow velocities capable of clast transport according to various transport modes (sliding, overturning, lifting), calculated using the hydrodynamic flow transport equations of Nandasena et al. (2011); Nandasena and Tanaka, (2013). The minimum flow velocities (MFVs) required to set boulders in motion are the velocity values at the base of each colour band corresponding to the different modes of transport. It is likely that overturning (**Eq. 4**) was the transport mode necessary to move boulders from their source locations across the rugose and karstified surface of the Dahu Reef platform. Lifting (**Eq. 3**) is assumed to have been necessary to stack together the limestone clasts forming the SBCs viewed in **Figure 9**. Clasts exhibiting stacking (some with clear imbrication, see text) are identified by (S).

the boulder was transported in a southwest direction for at least 30 m, and that the clast was overturned during movement. This inferred boulder transport direction may explain the lack of boulder reworking on SE-facing Dahu Reef during Typhoon Tembin, because the strongest waves approached the island from the northeast. The buoy record showed the wave direction ranged from 78 to 146° (NE to SE) when significant wave height was highest (H_s >6 m) (personal communication with the Water Resources Agency of the Ministry of Economic Affairs, Taiwan). Overall, therefore, it is evident that the great majority of existing coastal boulder fields on Dahu Reef were not reorganised by Typhoon Tembin-generated waves.

Inferred Wave Conditions of Palaeo-HEW Events

As described in *Estimating (Palaeo)Wave-Generated Flow Characteristics* section, the application of published flow transport equations by Nandasena et al. (2011); Nandasena and Tanaka, (2013) allowed calculation of minimum flow velocities (MFVs) required to initiate coastal boulder movement (**Figure 12**). This method is a surrogate for estimating the magnitudes of past typhoons. All reef-derived limestone clasts are assumed to have been either overturned (possibly lifted) from their original sources at the reef edge, karstic depressions or cross-cutting reef channels, onto the Dahu Reef platform. Two volcanic clasts where past wave transport is certain (**Figure 7**) are also included in calculations. For limestone clasts that are stacked up against each other (**Figure 9**), lifting is presumed necessary for stacking, and likewise for the slab that was lifted out from the concrete apron of the boat ramp (**Figures 11A,B**) by Typhoon Tembin. Based on the assumption of overturning for limestone and concrete clasts moved during Typhon Tembin, MFVs were 3.2–5.1 m/s, whereas 5.1 m/s was required for lifting of the slab shown in **Figures 11A,B**. In contrast, however, palaeo-HEW events were stronger. MFVs of 4.3–7.6 m/s are required to overturn the limestone clasts, with higher MFVs of 5.2–8.6 m/s needed for the two volcanic clasts for which overturning is certain (**Figure 7**). For the limestone clasts within the SBCs (**Figure 9**), where (partial) lifting was presumed necessary, MFVs of 8.3–13.8 m/s would have been required.

DISCUSSION

Origin of Imbrication: The Importance of Local Reef Geomorphology

A prominent characteristic of the boulder field on Dahu Reef is the presence of imbricated boulders among stacks of mixed lithology. In coastal boulder fields, imbrication always begins with an obstacle at the landward end (Scheffers and Kinis, 2014). The obstacle can be a large boulder, a stable ridge, or a steeper slope. Here, boulder imbrication is possible because of 1) a slight depression (0.5–1 m) in the reef platform, 2) large volcanic clasts, possibly products of rockfalls, acting as "stoppers" for wave-transported limestone boulders to lean against, 3) the presence of multiple flat-shaped boulders (**Figures 6**, **9**; a- and b-axes significantly longer than c-axes). The imbricated limestone boulders show fairly regular orientation, notwithstanding the irregular reef surface, with ab-planes dipping toward the source of the flow. Imbrication represents a stable pattern for coastal boulders, thereby inhibiting further movement. Other boulders were also stoppered by the surface roughness of the karstified reef platform. More boulders subsequently stack against the landward-most boulders to create trains of SBCs.

On a volcanic island like Ludao, detached volcanic boulders could have come from cliff collapse or rockfall. However, imbrication of reef-derived limestone boulders is clear evidence that wave action must have played a role in their deposition at current locations. The inclined position of imbricated boulders also implies that clasts were at least partially lifted and overturned in the flow, as sliding transport cannot produce imbricate structures. Furthermore, the overlap of boulders forming SBCs is indicative of both wave-transport direction and the sequence of boulder deposition. Such features are therefore valuable for inferring several characteristics of the high-energy waves that once transported the clasts.

Imbricate patterns usually form in places with numerous clasts of similar sizes, because the likelihood of imbrication is determined by the degree of sediment sorting (Galvin, 1978). Imbricated boulders resulting from high-energy waves have mostly been reported on well-jointed rocky coasts, where clasts of similar sizes are in abundance. In contrast, discovering imbricated large boulders on Ludao was unexpected, considering the low clast count (fewer than 50 large boulders at our study site) and the lack of jointing in the reef limestone. This leads us to deduce that reef morphology is the controlling influence here on boulder clustering, stacking and imbrication. Similarly, the dip angle of imbricated clasts is not wholly controlled by the flow velocity as commonly observed, but by the topography that contributes to platform surface roughness and the shape of existing boulders in a stack.

Importantly, the remnant spur-and-groove features on Dahu Reef, extending landward of the modern living reef edge onto the Holocene platform, are thought to be critical. They provide both source sites for clast excavation and topographic lows for boulder clustering. The elongated, narrow, shore-perpendicular grooves allow fast-moving flows to funnel onto the Holocene reef, resulting in amplified hydrodynamic forces that are capable of quarrying and lifting boulders from back-reef locations, rather than the modern seaward reef edge. This observation suggests that forces from localised water incursion are sensitive to reef-platform morphology and are capable of moving large boulders appreciable distances. Similar results were found by Goto et al. (2010a) on the Thailand coast where the spatial distribution of boulders deposited by the 2004 Indian Ocean tsunami was explained according to the localised behaviour of the tsunami, as affected by the local topography.

Coastal Exposure on Ludao

Typhoons generally travel westward-to-northward in the NW Pacific basin. As typhoons approach Taiwan, they sometimes weaken because of airflow disturbance by the island's mountainous terrain. Ludao and Lanyu islands, however, as offshore islands lying 30–70 km east of the main island of Taiwan, are exposed to the full brunt of extreme-wave events generated in the Pacific Ocean, making them ideal locations for study. Being popular tourist destinations, they also deserve attention for disaster risk reduction and management. Our post-event fieldwork on Ludao following the passage of Typhoon Tembin in 2012 revealed several coastal boulders of up to 3.4 m^3 (8.1 t) were transported by Tembin-associated storm waves. Estimated MFVs generated lie in the conservative range 3.2–5.1 m/s, owing to the lack of evidence for boulder saltation or suspension in the flow. These flow magnitudes are similar to clast-inferred MFVs of 3–6 m/s on mainland Taiwan's eastern beaches when Typhoon Soudelor made landfall in 2015 (Huang et al., 2020), although the availability of only small (<1 t) metamorphic boulders there may have underestimated the wave-transport capabilities of that typhoon.

Nevertheless, compared to these modern events, the presence of larger wave-transported boulders on Dahu Reef provides evidence that considerably stronger coastal inundation event(s) have impacted Ludao before 1979, the year of the earliest aerial photo we obtained. Unfortunately, the ages of these past inundation events are unknown, as the boulder deposits are unsuitable for age-dating. Their undetermined source locations mean that the age of coral limestone fabric would not be representative of boulder dislodgement timing, as explained in Lau et al. (2018). The clustering of boulders suggests a potentially complex boulder remobilisation history, such that cosmogenic nuclide exposure dating (Rixhon, 2020) is also inappropriate for this dataset.

Even in the absence of age-dating, however, this study adds another useful dataset of storm-wave transported boulders to the growing number of similar studies on tropical Asia-Pacific coasts (**Table 3**). Our boulder-inferred flow velocities, estimated for palaeo-HEW events that have affected eastern Ludao, compare favourably with the findings from other storm-prone locations. Here, the availability of denser volcanic boulders on Dahu Reef with evidence of wave overturning allows us to include them in the dataset. Non-carbonate boulders are uncommon on coral reef platforms elsewhere, unless reefs are in juxtaposition with bedrock cliffs or outcrops of other rock types. At Dahu Reef, the reef platform is relatively narrow, extending less than 200 m from the toe of surrounding hills, and there are outcrops of volcanic breccia

TABLE 3 | Comparison of onshore flow velocities generated by typhoons and tropical cyclones across the Asia–Pacific region, as modelled from the characteristics of wave-transported coastal boulders.

Country	Area	Island studied	Specific event if named	MFV (m/s)	Main geomorphic setting of coastal boulders	Principal boulder lithology	Key References
Taiwan	Taitung County	Lanyu	Past typhoons (inferred)	1.4–16.9	Holocene reef platform	Limestone	Nakamura et al. (2014)
"	"	Ludao	"	3.1–5.9	Beach	Calcarenite slabs excavated from beachrock exposure	Lau *et al.* (2015)
"	"	"	Typhoon Tembin 2012	3.2–5.1[a]	Holocene reef platform and boat ramp	Limestone and concrete	This study
"	"	"	Past typhoons (inferred)	4.3–13.8[b]	Holocene reef platform	Limestone	"
"	"	"	"	5.2–8.6[a]	"	Volcanic	"
"	Hualien County	Taiwan	Typhoon Soudelor 2015	3–6	Beach	Metamorphic excavated from revetment	Huang et al. (2020)
French Polynesia	Society Islands	Huahine	Cyclone Oli 2010	3.1–5.3	Beach	Calcarenite slabs excavated from beachrock exposure	Etienne (2012)
Fiji	Northern Division	Taveuni	Past cyclones (inferred)	3.5–15.0[c]	Fringing reef platforms	Limestone (coral)	Terry and Lau (2018)
"	"	"	Cyclone Tomas 2010	5.1–11.7[c]	"	"	"
"	"	"	Cyclone Winston 2016	5.8–13.8[c]	"	"	"
The Philippines	Eastern Samar Province	Samar	Typhoon Haiyan 2013	8.9–9.6	Various: rocky coast, beach, emerged carbonate platforms	Limestone	May et al. (2015)
"	"	Calicoan	"	5–9	Low limestone cliffs	Limestone	Kennedy et al. (2017)
Thailand	Gulf of Thailand	Ko Samui	Past typhoons (inferred)	2.3–4.6	Holocene fringing reef platform; slightly emerged	Limestone (coral)	Terry et al. (2016)
"	"	"	"	5.1–8.6[d]	Talus slopes	"	"
	Bay of Bangkok	Ko Larn	Past typhoons (inferred)	1.9–5.3	Talus slopes	Limestone (coral)	Terry et al. (2015)
"	"	Ko Phai and Ko Khang Khao	"	3.0–5.5[a]	"	"	Terry et al. (2018)
"	"	Ko Larn	"	2.9–7.3[e]	Shore platforms	Sandstone	Terry and Goff (2019)

[a]*Ranges given are for the overturning mode of transport.*
[b]*Ranges given are for the overturning mode of transport, or lifting for clasts that have been stacked up against each other.*
[c]*Ranges given are for the lifting mode of transport for limestone boulders assumed to have been quarried originally from the reef edge.*
[d]*Ranges given are for the lifting mode of transport for limestone boulders carried up and deposited among talus slopes.*
[e]*Ranges given are for the sliding and overturning modes of transport for remobilization of boulders sourced from rockfall.*

projecting through the limestone reef, providing a local source of non-carbonate boulders, adding to the reef-derived limestone boulders.

Besides typhoons, eastern Taiwan is also potentially at risk of tsunami hazards (Ota, 2012; Matta et al., 2013). Numerical simulation has shown that a Mw 8.7 earthquake from the Ryukyu Trench may result in run-up heights up to 15 m on the east coast of Lanyu, the offshore island neighbouring Ludao (Ando et al., 2013; Nakamura et al., 2014). Another model to simulate tsunami amplitude initiated by a Mw 8.15 earthquake at the same trench estimated a maximum wave height of 2.04 m at northern Ludao (Sun et al., 2018). In spite of these projections, however, none of the boulder deposits we examined on Dahu Reef show indication of long-period tsunami wave transport. The major depositional cluster with the largest stacked clasts is found within 100 m of the reef edge, and all boulders conform to size–distance distribution patterns that can be explained by large storm waves. Overall, therefore, we find no geological evidence of tsunamis on eastern Ludao, notwithstanding the simulated tsunami risks. This contrasts with the findings of Ota et al. (2015) from work on neighbouring Lanyu Island. There, large coastal limestone boulders (up to 234 t) were interpreted as palaeotsunami deposits. However, the difference with the Lanyu boulder sites, compared to our Ludao site, is that they face north towards the Ryukyu Trench, which is the main regional candidate for tsunami generation.

CONCLUSION

Ludao Island, a small offshore island in southern Taiwan, is uniquely exposed to Pacific typhoons. On the emerged Holocene limestone platform of Dahu Reef in SE Ludau, past high-energy events have created coastal boulder fields of mixed limestone and volcanic lithologies. Several individual boulders are of megaclast dimensions. From coastal boulder measurements and boulder-inferred hydrodynamic estimations, damaging Typhoon Tembin in 2012, which struck Ludao twice by following a looping track, generated onshore flow velocities of 3.2–5.1 m/s. However, these values were notably exceeded by more powerful typhoons in the past, with inferred

flow velocities of 4.3–13.8 m/s. These past storms were capable of clustering, stacking and imbricating very large clasts (10^3–10^4 kg).

The presence of stacked boulder clusters (SBCs) on Ludao is particularly important, because SBCs indicate that partial lifting (and overturning) must have occurred during wave-induced clast transport. Reef geomorphology has been shown to be a key controlling influence on SBC formation. The existence of narrow shore-perpendicular channels that cut across the Holocene reef are inherited (relict) spur-and-groove features, similar to the modern morphology that characterizes the living seaward reef margin. The singular location of SBC-styles of large clast deposition around the head of such features suggests that relict channels are able to confine and amplify the force of shoreward incursion in high velocity jet-like flows. Previous assertions that depositional features such as clustering, stacking and imbrication of very large coastal boulders are possibly key indicators of past tsunami events have been challenged. Our findings in Ludao's typhoon-dominated environment likewise indicate that invoking a tsunami explanation is not necessary to account for the origin of SBCs and comparable coastal deposits.

DATA AVAILABILITY STATEMENT

The raw data supporting the conclusion of this article will be made available by the authors, without undue reservation.

AUTHOR CONTRIBUTIONS

AS, JT, and AL participated in fieldwork. Y-AL analyzed typhoon tracks. KN analyzed air photo imagery. JT analyzed field data. JT and AL prepared the figures. JT and AL wrote the draft manuscript. AS edited the manuscript.

FUNDING

JT acknowledges research support from the National University of Singapore (ARF grant FY2012-FRC2-005) and Zayed University (RIF grant R19088). AL and AS acknowledge research support from the National University of Singapore and Earth Observatory of Singapore (EOS) at Nanyang Technological University. This paper is EOS contribution 416.

ACKNOWLEDGMENTS

Our appreciation is extended to Executive Yuan of the Aerial Survey Office, Forestry Bureau, Council of Agriculture, Taiwan, for providing archived historical aerial photographs. Lee Kheng (Singapore) and Maitha Eisa Almeer (Dubai) kindly assisted with preparing early drafts of **Figure 2**.

REFERENCES

Ando, M., Nakamura, M., and Lin, C.-H. (2013). Tsunami Folklore and Possible Tsunami Source on the Eastern Coast of Taiwan. *Terr. Atmos. Ocean. Sci.* 24, 951–961. doi:10.3319/tao.2013.07.12.01(t)

Bishop, P., and Hughes, M. (1989). Imbricate and Fitted Fabrics in Coastal boulder Deposits on the Australian East Coast. *Geol.* 17, 544–547. doi:10.1130/0091-7613(1989)017<0544:iaffic>2.3.co;2

Blott, S. J., and Pye, K. (2008). Particle Shape: a Review and New Methods of Characterization and Classification. *Sedimentology* 55, 31–63. doi:10.1111/j.1365-3091.2007.00892.x

Bryant, E. A., and Nott, J. (2001). Geological Indicators of Large Tsunami in Australia. *Nat. Hazards* 24, 231–249. doi:10.1023/a:1012034021063

Bryant, E. (2014). *Tsunami: The Underrated Hazard*. 3rd edition. Cham: Springer, 242.

Central Weather Bureau (CWB),(2013a). Wave Statistics. Available at: http://www.cwb.gov.tw/V7e/climate/marine_stat/wave.htm. (Accessed August, 2014).

Central Weather Bureau (CWB) (2013b). Typhoon's Impact on Taiwan - How many Typhoons Have Invaded Taiwan Historically? Which Month Has the Peak Value in Frequency? Available at: http://www.cwb.gov.tw/V7e/knowledge/encyclopedia/ty014.htm. (Accessed August, 2014).

Central Weather Bureau (CWB) (2013c). Typhoon's Impact on Taiwan - How many Typhoons Hit Taiwan Historically? Which Month of the Year Is the Most Frequently Impacted? (歷年有多少次颱風侵襲臺灣?以哪個月份最多?). (in Chinese). Available at: http://www.cwb.gov.tw/V7/knowledge/encyclopedia/ty038.htm. (Accessed August, 2014).

Central Weather Bureau (CWB) (2013d). Typhoon's Impact on Taiwan - How many Typhoon Landfalls Have Been on Taiwan? Which Spot Has the Most Landfalls? (颱風在臺灣登陸多少次?以何處登陸次數較多?). (in Chinese). Available at: http://www.cwb.gov.tw/V7/knowledge/encyclopedia/ty040.htm. (Accessed August, 2014).

Chan, J. C. L. (1985). Tropical Cyclone Activity in the Northwest Pacific in Relation to the El Niño/Southern Oscillation Phenomenon. *Mon. Wea. Rev.* 113, 599–606. doi:10.1175/1520-0493(1985)113<0599:tcaitn>2.0.co;2

Conybeare, C. E. B., and Crook, K. A. W. (1982). *Manual of Sedimentary Structures*, 102. Canberra: Bureau of Mineral Resources, Geology and Geophysics, Australian Government Publishing Service, 327pp. BMR Bulletin.

Cox, R., Zentner, D. B., Kirchner, B. J., and Cook, M. S. (2012). Boulder Ridges on the Aran Islands (Ireland): Recent Movements Caused by Storm Waves, Not Tsunamis. *J. Geology* 120, 249–272. doi:10.1086/664787

Cox, R., O'Boyle, L., and Cytrynbaum, J. (2019). Imbricated Coastal boulder Deposits Are Formed by Storm Waves, and Can Preserve a Long-Term Storminess Record. *Sci. Rep.* 9, 10784. doi:10.1038/s41598-019-47254-w

Dewey, J. F., Goff, J., and Ryan, P. D. (2021). The Origins of marine and Non-marine boulder Deposits: a Brief Review. *Nat. Hazards* 109, 1981–2002. doi:10.1007/s11069-021-04906-3

Doong, D., Chuang, L. Z. H., Kao, C. C., Lin, Y., and Jao, K. (2009). *Statistics of Buoy-Observed Waves during Typhoons at Taiwanese Waters from 1997 to 2008. OCEANS 2009, MTS/IEEE Biloxi-Marine Technology for Our Future: Global and Local Challenges*. Mississippi: Biloxi, 1–7.

Engel, M., and May, S. M. (2012). Bonaire's boulder fields Revisited: Evidence for Holocene Tsunami Impact on the Leeward Antilles. *Quat. Sci. Rev.* 54, 126–141. doi:10.1016/j.quascirev.2011.12.011

Erdmann, W., Kelletat, D., Scheffers, A., and Haslett, S. K. (2015). *Origin and Formation of Coastal boulder Deposits at Galway Bay and the Aran Islands, Western Ireland*. Cham: Springer.

Erdmann, W., Kelletat, D., and Scheffers, A. (2018). Boulder Transport by Storms - Extreme-Waves in the Coastal Zone of the Irish West Coast. *Mar. Geology* 399, 1–13. doi:10.1016/j.margeo.2018.02.003

Etienne, S., and Paris, R. (2010). Boulder Accumulations Related to Storms on the South Coast of the Reykjanes Peninsula (Iceland). *Geomorphology* 114, 55–70. doi:10.1016/j.geomorph.2009.02.008

Etienne, S., and Terry, J. P. (2012). Coral Boulders, Gravel Tongues and Sand Sheets: Features of Coastal Accretion and Sediment Nourishment by Cyclone Tomas (March 2010) on Taveuni Island, Fiji. *Geomorphology* 175-176, 54–65. doi:10.1016/j.geomorph.2012.06.018

Etienne, S. (2012). "Marine Inundation Hazards in French Polynesia: Geomorphic Impacts of Tropical Cyclone Oli in February 2010," in *Natural Hazards in the*

Asia–Pacific Region: Recent Advances and Emerging Concepts. Editors J. P. Terry and J. Goff (Geological Society of London, Special Publication), 361, 21–39. doi:10.1144/sp361.4

Felton, E. A., and Crook, K. A. W. (2003). Evaluating the Impacts of Huge Waves on Rocky Shorelines: an Essay Review of the Book 'Tsunami - the Underrated Hazard'. *Mar. Geology.* 197, 1–12. doi:10.1016/s0025-3227(03)00086-0

Frohlich, C., Hornbach, M. J., Taylor, F. W., Shen, C.-C., Moala, A., Morton, A. E., et al. (2009). Huge Erratic Boulders in Tonga Deposited by a Prehistoric Tsunami. *Geology* 37, 131–134. doi:10.1130/g25277a.1

Galvin, C. (1978). "Imbrication and Flow-Oriented Clasts," in *Sedimentology. Encyclopedia of Earth Science* (Berlin, Heidelberg: Springer), 601–604. doi:10.1007/3-540-31079-7_116

Geological Map of Taiwan (1986). *Taiwan 1:50,000 Scale Geological Maps*. New Taipei City: Central Geological Survey, Ministry of Economic Affairs.

Gienko, G. A., and Terry, J. P. (2014). Three-dimensional Modeling of Coastal Boulders Using Multi-View Image Measurements. *Earth Surf. Process. Landforms* 39, 853–864. doi:10.1002/esp.3485

Goto, K., Okada, K., and Imamura, F. (2010a). Numerical Analysis of boulder Transport by the 2004 Indian Ocean Tsunami at Pakarang Cape, Thailand. *Mar. Geology.* 268, 97–105. doi:10.1016/j.margeo.2009.10.023

Goto, K., Shinozaki, T., Minoura, K., Okada, K., Sugawara, D., and Imamura, F. (2010b). Distribution of Boulders at Miyara Bay of Ishigaki Island, Japan: a Flow Characteristic Indicator of Tsunami and Storm Waves. *Isl. Arc.* 19, 412–426. doi:10.1111/j.1440-1738.2010.00721.x

Hall, A. M., Hansom, J. D., Williams, D. M., and Jarvis, J. (2006). Distribution, Geomorphology and Lithofacies of Cliff-Top Storm Deposits: Examples from the High-Energy Coasts of Scotland and Ireland. *Mar. Geology.* 232, 131–155. doi:10.1016/j.margeo.2006.06.008

Hall, A. M., Hansom, J. D., and Williams, D. M. (2010). Wave-emplaced Coarse Debris and Megaclasts in Ireland and Scotland: Boulder Transport in a High-Energy Littoral Environment: A Discussion. *J. Geology* 118, 699–704. doi:10.1086/656357

Hansom, J. D., and Hall, A. M. (2009). Magnitude and Frequency of Extra-tropical North Atlantic Cyclones: A Chronology from Cliff-Top Storm Deposits. *Quat. Int.* 195, 42–52. doi:10.1016/j.quaint.2007.11.010

Hearty, P. J., and Tormey, B. R. (2017). Sea-level change and superstorms; geologic evidence from the last interglacial (MIS 5e) in the Bahamas and Bermuda offers ominous prospects for a warming Earth. *Mar. Geology* 390, 347–365. doi:10.1016/j.margeo.2017.05.009

Huang, S.-Y., Yen, J.-Y., Wu, B.-L., and Shih, N.-W. (2020). Field Observations of Sediment Transport across the Rocky Coast of East Taiwan: Impacts of Extreme Waves on the Coastal Morphology by Typhoon Soudelor. *Mar. Geology.* 421, 106088. doi:10.1016/j.margeo.2019.106088

Huang, T.-T. (2020). *Overtourism a Blessing and Curse for Taiwan's Outlying Islands*. Taiwan News. Available at: https://www.taiwannews.com.tw/en/news/3978545 (Accessed 08 01, 2020).

Inoue, S., Kayanne, H., Matta, N., Chen, W. S., and Ikeda, Y. (2011). Holocene Uplifted Coral Reefs in Lanyu and Lutao Islands to the Southeast of Taiwan. *Coral Reefs* 30, 581–592. doi:10.1007/s00338-011-0783-x

Iwai, S., Goto, K., and Ishizawa, T. (2019). A Gigantic boulder Transported by the 2011 Tohoku-oki Tsunami. *Isl. Arc.* 28, e12321. doi:10.1111/iar.12321

Jones, B., and Hunter, I. G. (1992). Very Large Boulders on the Coast of Grand Cayman, the Effects of Giant Waves on Rocky Shorelines. *J. Coastal Res.* 8, 763–774.

Juang, W.-S., and Chen, J.-C. (1990). Geochronology and Chemical Variations of Volcanic Rocks along the Arc-Continent Collision Zone in Eastern Taiwan. *Bull. Natl. Mus. Nat. Sci.* 2, 89–118.

Kato, Y., and Kimura, M. (1983). Age and Origin of So-Called 'Tsunamiishi', Ishigaki Island, Okinawa Prefecture. *Jour. Geol. Soc. Jpn.* 89, 471–474. doi:10.5575/geosoc.89.471

Kennedy, D. M., Tannock, K. L., Crozier, M. J., and Rieser, U. (2007). Boulders of MIS 5 Age Deposited by a Tsunami on the Coast of Otago, New Zealand. *Sediment. Geology* 200, 222–231. doi:10.1016/j.sedgeo.2007.01.005

Kennedy, A. B., Mori, N., Yasuda, T., Shimozono, T., Tomiczek, T., Donahue, A., et al. (2017). Extreme Block and boulder Transport along a Cliffed Coastline (Calicoan Island, Philippines) during Super Typhoon Haiyan. *Mar. Geology* 383, 65–77. doi:10.1016/j.margeo.2016.11.004

Kennedy, D. M., Woods, J. L. D., Naylor, L. A., Hansom, J. D., and Rosser, N. J. (2019). Intertidal boulder-based Wave Hindcasting Can Underestimate Wave Size: Evidence from Yorkshire, UK. *Mar. Geology.* 411, 98–106. doi:10.1016/j.margeo.2019.02.002

Lario, J., Spencer, C., Bardají, T., Marchante, Á., Garduño-monroy, V. H., Macias, J., et al. (2020). An Extreme Wave Event in Eastern Yucatán, Mexico: Evidence of a Palaeotsunami Event during the Mayan Times. *Sedimentology* 67, 1481–1504. doi:10.1111/sed.12662

Lau, A. Y. A., Terry, J. P., Switzer, A. D., and Pile, J. (2015). Advantages of Beachrock Slabs for Interpreting High-Energy Wave Transport: Evidence from Ludao Island in South-Eastern Taiwan. *Geomorphology* 228, 263–274. doi:10.1016/j.geomorph.2014.09.010

Lau, A. Y. A., Terry, J. P., Ziegler, A., Pratap, A., and Harris, D. (2018). Boulder Emplacement and Remobilisation by Cyclone and Submarine Landslide Tsunami Waves Near Suva City, Fiji. *Sediment. Geology* 364, 242–257. doi:10.1016/j.sedgeo.2017.12.017

Lee, Y.-S., Liou, Y.-A., Liu, J.-C., Chiang, C.-T., and Yeh, K.-D. (2017). Formation of Winter Supertyphoons Haiyan (2013) and Hagupit (2014) through Interactions with Cold Fronts as Observed by Multifunctional Transport Satellite. *IEEE Trans. Geosci. Remote Sens.* 55, 3800–3809. doi:10.1109/tgrs.2017.2680418

Li, C. H., Hsu, M. K., Cheng, W. B., Hsiao, S. C., and Lin, Q. L. (2006). *Preliminary Research on the Development of Tsunami Warning System at Northeastern Taiwan*. Taipei: Central Weather Bureau, Taiwan.

Liou, Y.-A., Liu, J.-C., Wu, M.-X., Lee, Y.-J., Cheng, C.-H., Kuei, C.-P., et al. (2016). Generalized Empirical Formulas of Threshold Distance to Characterize Cyclone-Cyclone Interactions. *IEEE Trans. Geosci. Remote Sens.* 54, 3502–3512. doi:10.1109/tgrs.2016.2519538

Liou, Y.-A., Liu, J.-C., Liu, C. P., and Liu, C.-C. (2018). Season-dependent Distributions and Profiles of Seven Super-typhoons (2014) in the Northwestern Pacific Ocean from Satellite Cloud Images. *IEEE Trans. Geosci. Remote Sens.* 56, 2949–2957. doi:10.1109/tgrs.2017.2787606

Liou, Y.-A., Liu, J.-C., Liu, C.-C., Chen, C.-H., Nguyen, K.-A., and Terry, J. P. (2019). Consecutive Dual-Vortex Interactions between Quadruple Typhoons Noru, Kulap, Nesat and Haitang during the 2017 North Pacific Typhoon Season. *Remote Sens.* 11, 1843. doi:10.3390/rs11161843

Liu, J.-C., Liou, Y.-A., Wu, M.-X., Lee, Y.-J., Cheng, C.-H., Kuei, C-P., et al. (2015). Analysis of Interactions Among Two Tropical Depressions and Typhoons Tembin and Bolaven (2012) in Pacific Ocean by Using Satellite Cloud Images. *IEEE Trans. Geosci. Remote Sens.* 53, 1934–1402. doi:10.1109/tgrs.2014.2339220

Master, S. (2014). "A Note on Imbricated Granite Boulders on NW Penang Island, Malaysia: Tsunami or Storm Origin?" in *Tsunami Events And Lessons Learned: Environmental And Societal Significance, Advances in Natural and Technological Hazards Research 35*. Editors Y. A. Kontar, Y. Santiago-Fandiño, and T. Takahashi (Dordrecht: Springer), 225–241. doi:10.1007/978-94-007-7269-4_12

Matta, N., Ota, Y., Chen, W.-S., Nishikawa, Y., Ando, M., and Chung, L.-H. (2013). Finding of Probable Tsunami Boulders on Jiupeng Coast in southeastern Taiwan. *Terr. Atmos. Ocean. Sci.* 24, 159–163. doi:10.3319/tao.2012.09.14.01(tt)

Mattioli, M., De Masi, G., and Drago, M. (2019). Evaluating Extreme Cyclonic Sea States. *Ocean Eng.* 194, 106639. doi:10.1016/j.oceaneng.2019.106639

May, S. M., Engel, M., Brill, D., Cuadra, C., Lagmay, A. M. F., Santiago, J., et al. (2015). Block and boulder Transport in Eastern Samar (Philippines) during Supertyphoon Haiyan. *Earth Surf. Dynam.* 3, 543–558. doi:10.5194/esurf-3-543-2015

Mhammdi, N., Medina, F., Kelletat, D., Ahmamou, M., and Aloussi, L. (2008). Large Boulders along the Rabat Coast (Morocco); Possible Emplacement by the November, 1st, 1755 A.D. Tsunami. *Sci. Tsunami Hazards* 27, 17–30.

Morton, R. A., Richmond, B. M., Jaffe, B. E., and Gelfenbaum, G. (2006). Reconnaissance Investigation of Caribbean Extreme Wave Deposits - Preliminary Observations, Interpretations, and Research Directions. Open-file report 1293. USGS, 46. doi:10.3133/ofr20061293

Mottershead, D., Bray, M., Soar, P., and Farres, P. J. (2014). Extreme Wave Events in the Central Mediterranean: Geomorphic Evidence of Tsunami on the Maltese Islands. *zfg* 58, 385–411. doi:10.1127/0372-8854/2014/0129

Mottershead, D. N., Bray, M. J., and Soar, P. J. (2017). "Tsunami Landfalls in the Maltese Archipelago: Reconciling the Historical Record with Geomorphological Evidence," in *Tsunamis: Geology, Hazards and Risks*. Editors E. M. Scourse, N. A. Chapman, D. R. Tappin, and S. R. Wallis (Geological Society, London, Special Publications), 456, 127–141. doi:10.1144/sp456.8

Nakamura, M., Arashiro, Y., and Shiga, S. (2014). Numerical Simulations to Account for boulder Movements on Lanyu Island, Taiwan: Tsunami or Storm? *Earth, Planets Space* 66, 128. doi:10.1186/1880-5981-66-128

Nandasena, N. A. K., and Tanaka, N. (2013). Boulder Transport by High Energy: Numerical Model-Fitting Experimental Observations. *Ocean Eng.* 57, 163–179. doi:10.1016/j.oceaneng.2012.09.012

Nandasena, N. A. K., Paris, R., and Tanaka, N. (2011). Reassessment of Hydrodynamic Equations: Minimum Flow Velocity to Initiate boulder Transport by High Energy Events (Storms, Tsunamis). *Mar. Geology.* 281, 70–84. doi:10.1016/j.margeo.2011.02.005

Noormets, R., Felton, E. A., and Crook, K. A. W. (2002). Sedimentology of Rocky Shorelines: 2. Shoreline Megaclasts on the North Shore of Oahu, Hawaii: Origins and History. *Sediment. Geology.* 150, 31–45. doi:10.1016/s0037-0738(01)00266-4

Noormets, R., Crook, K., and Felton, E. (2004). Sedimentology of Rocky Shorelines: 3.Hydrodynamics of Megaclast Emplacement and Transport on a Shore Platform, Oahu, Hawaii. *Sediment. Geology.* 172, 41–65. doi:10.1016/s0037-0738(04)00235-0

Nott, J. (1997). Extremely High-Energy Wave Deposits inside the Great Barrier Reef, Australia: Determining the Cause-Tsunami or Tropical Cyclone. *Mar. Geology.* 141, 193–207. doi:10.1016/s0025-3227(97)00063-7

Nott, J. (2003). Waves, Coastal boulder Deposits and the Importance of the Pre-transport Setting. *Earth Planet. Sci. Lett.* 210, 269–276. doi:10.1016/s0012-821x(03)00104-3

Nott, J. (2004). The Tsunami Hypothesis-Comparisons of the Field Evidence against the Effects, on the Western Australian Coast, of Some of the Most Powerful Storms on Earth. *Mar. Geology.* 208, 1–12. doi:10.1016/j.margeo.2004.04.023

Ota, Y., Shyu, J. B. H., Wang, C.-C., Lee, H.-C., Chung, L.-H., and Shen, C.-C. (2015). Coral Boulders along the Coast of the Lanyu Island, Offshore southeastern Taiwan, as Potential Paleotsunami Records. *J. Asian Earth Sci.* 114, 588–600. doi:10.1016/j.jseaes.2015.08.001

Ota, Y. (2012). Geological Data for Possible Paleotsunami at the Eastern Coast of Taiwan. *Quat. Int.* 279-280, 362–363. doi:10.1016/j.quaint.2012.08.1103

Paris, R., Naylor, L. A., and Stephenson, W. J. (2011). Boulders as a Signature of Storms on Rock Coasts. *Mar. Geology.* 283, 1–11. doi:10.1016/j.margeo.2011.03.016

Pepe, F., Corradino, M., ParrinoBesio, N. G., Besio, G., Presti, V. L., Renda, P., et al. (2018). Boulder Coastal Deposits at Favignana Island Rocky Coast (Sicily, Italy): Litho-Structural and Hydrodynamic Control. *Geomorphology* 303, 191–209. doi:10.1016/j.geomorph.2017.11.017

Rixhon, G. (2020). "Cosmogenic Nuclide Dating of Coarse Clasts," in *Geological Records of Tsunamis and Other Extreme Waves*. Editors M. Engel, J. Pilarczyk, S. M. May, D. Brill, and E. Garrett (Elsevier), 761–775. doi:10.1016/b978-0-12-815686-5.00035-3

Roig-Munar, F. X., Vilaplana, J. M., Rodríguez-Perea, A., Martín-Prieto, J. Á., and Gelabert, B. (2018). Tsunamis Boulders on the Rocky Shores of Minorca (Balearic Islands). *Nat. Hazards Earth Syst. Sci.* 18, 1985–1998. doi:10.5194/nhess-18-1985-2018

Scheffers, A. M., and Kinis, S. (2014). Stable Imbrication and Delicate/unstable Settings in Coastal boulder Deposits: Indicators for Tsunami Dislocation? *Quat. Int.* 332, 73–84. doi:10.1016/j.quaint.2014.03.004

Scheffers, A., Scheffers, S., Kelletat, D., and Browne, T. (2009). Wave-Emplaced Coarse Debris and Megaclasts in Ireland and Scotland: Boulder Transport in a High-Energy Littoral Environment. *J. Geology.* 117, 553–573. doi:10.1086/600865

Scheffers, A. (2004). Tsunami Imprints on the Leeward Netherlands Antilles (Aruba, Curaçao, Bonaire) and Their Relation to Other Coastal Problems. *Quat. Int.* 120, 163–172. doi:10.1016/j.quaint.2004.01.015

Scicchitano, G., Pignatelli, C., Spampinato, C. R., Piscitelli, A., Milella, M., Monaco, C., et al. (2012). Terrestrial Laser Scanner Techniques in the Assessment of Tsunami Impact on the Maddalena peninsula (South-eastern Sicily, Italy). *Earth Planet. Sp* 64, 889–903. doi:10.5047/eps.2011.11.009

Shah-hosseini, M., Morhange, C., Naderi Beni, A., Marriner, N., Lahijani, H., Hamzeh, M., et al. (2011). Coastal Boulders as Evidence for High-Energy Waves on the Iranian Coast of Makran. *Mar. Geology.* 290, 17–28. doi:10.1016/j.margeo.2011.10.003

Shen, C.-C., Wu, C.-C., Dai, C.-F., and Gong, S.-Y. (2018). Variable Uplift Rate through Time: Holocene Coral Reef and Neotectonics of Lutao, Eastern Taiwan. *J. Asian Earth Sci.* 156, 201–206. doi:10.1016/j.jseaes.2018.01.016

Sun, Y.-S., Chen, P.-F., Chen, C.-C., Lee, Y.-T., Ma, K.-F., and Wu, T.-R. (2018). Assessment of the Peak Tsunami Amplitude Associated with a Large Earthquake Occurring along the Southernmost Ryukyu Subduction Zone in the Region of Taiwan. *Nat. Hazards Earth Syst. Sci.* 18, 2081–2092. doi:10.5194/nhess-18-2081-2018

Sussmilch, C. A. (1912). Note on Some Recent marine Erosion at Bondi. *J. Proc. R. Soc. New South Wales* 46, 155–158.

Switzer, A. D., and Burston, J. M. (2010). Competing Mechanisms for boulder Deposition on the Southeast Australian Coast. *Geomorphology* 114, 42–54. doi:10.1016/j.geomorph.2009.02.009

Terry, J. P., and Goff, J. (2019). Strongly Aligned Coastal Boulders on Ko Larn Island (Thailand): a Proxy for Past Typhoon-driven High-energy Wave Events in the Bay of Bangkok. *Geographical Res.* 57, 344–358. doi:10.1111/1745-5871.12342

Terry, J. P., and Lau, A. Y. A. (2018). Magnitudes of Nearshore Waves Generated by Tropical Cyclone Winston, the Strongest Landfalling Cyclone in South Pacific Records. Unprecedented or Unremarkable? *Sediment. Geology.* 364, 276–285. doi:10.1016/j.sedgeo.2017.10.009

Terry, J. P., and Malik, S. A. (2020). Reconsidering the Seawater-Density Parameter in Hydrodynamic Flow Transport Equations for Coastal Boulders. *New Zealand J. Geology. Geophys.* 63, 363–370. doi:10.1080/00288306.2020.1716815

Terry, J. P., Lau, A. Y. A., and Etienne, S. (2013). *Reef-Platform Coral Boulders: Evidence for High-Energy Marine Inundation Events on Tropical Coastlines*. Heidelberg: Springer, 105+xii.

Terry, J. P., Jankaew, K., and Dunne, K. (2015). Coastal Vulnerability to Typhoon Inundation in the Bay of Bangkok, Thailand? Evidence from Carbonate boulder Deposits on Ko Larn Island. *Estuarine, Coastal Shelf Sci.* 165, 261–269. doi:10.1016/j.ecss.2015.05.028

Terry, J. P., Oliver, G. J. H., and Friess, D. A. (2016). Ancient High-Energy Storm boulder Deposits on Ko Samui, Thailand, and Their Significance for Identifying Coastal hazard Risk. *Palaeogeogr. Palaeoclimatol. Palaeoecol.* 454, 282–293. doi:10.1016/j.palaeo.2016.04.046

Terry, J. P., Goff, J., and Jankaew, K. (2018). Major Typhoon Phases in the Upper Gulf of Thailand over the Last 1.5 Millennia, Determined from Coastal Deposits on Rock Islands. *Quat. Int.* 487, 87–98. doi:10.1016/j.quaint.2018.04.022

Terry, J. P., Karoro, R., Gienko, G. A., Wieczorek, M., and Lau, A. Y. A. (2021). Giant Palaeotsunami in Kiribati: Converging Evidence from Geology and Oral History. *Isl. Arc.* 30, e12417. doi:10.1111/iar.12417

Terry, J. P. (2005). Karst Distribution and Controls on Yoron-Jima, an Emerged Reef Island in Sub-tropical Japan. *J. Cave Karst Stud.* 67, 8–54.

Terry, J. P., and Goff, J. (2014). Megaclasts: proposed revised nomenclature at the coarse end of the Udden-Wentworth grain-size scale for sedimentary particles. *Journal of Sedimentary Research* 84, 192–197. doi:10.2110/jsr.2014.19

Weiss, R. (2012). The Mystery of Boulders Moved by Tsunamis and Storms. *Mar. Geology.* 295-298, 28–33. doi:10.1016/j.margeo.2011.12.001

Williams, D. M., and Hall, A. M. (2004). Cliff-top Megaclast Deposits of Ireland, a Record of Extreme Waves in the North Atlantic-storms or Tsunamis? *Mar. Geology.* 206, 101–117. doi:10.1016/j.margeo.2004.02.002

Yen, M.-C., and Chen, T.-C. (2000). Seasonal Variation of the Rainfall over Taiwan. *Int. J. Climatol.* 20, 803–809. doi:10.1002/1097-0088(20000615)20:7<803:aid-joc525>3.0.co;2-4

Young, R. W., Bryant, E. A., and Price, D. M. (1996). Catastrophic Wave (Tsunami?) Transport of Boulders in Southern New South Wales, Australia. *zfg* 40, 191–207. doi:10.1127/zfg/40/1996/191

Zingg, T. (1935). Beitrag zur schotteranalyse. *Schweiz. Mineral. und Petrogr. Mitt.* 15, 39–140.

Conflict of Interest: The authors declare that the research was conducted in the absence of any commercial or financial relationships that could be construed as a potential conflict of interest.